NACA RM E54E21

NACA

RESEARCH MEMORANDUM

INVESTIGATION OF MECHANICAL FASTENINGS FOR SOLID TURBINE BLADES MADE FROM DUCTILE MATERIALS

By André J. Meyer, Jr., Albert Kaufman, and W. C. Caywood

Lewis Flight Propulsion Laboratory
Cleveland, Ohio

NATIONAL ADVISORY COMMITTEE
FOR AERONAUTICS

WASHINGTON
August 2, 1954

NATIONAL ADVISORY COMMITTEE FOR AERONAUTICS

RESEARCH MEMORANDUM

INVESTIGATION OF MECHANICAL FASTENINGS FOR SOLID TURBINE BLADES MADE FROM DUCTILE MATERIALS

By André J. Meyer, Jr., Albert Kaufman, and W. C. Caywood

SUMMARY

Tensile specimens of fir-tree turbine blade root fastenings for three specific turbojet engines were tested to rupture. Short-time tests were conducted at various temperatures ranging from room temperature to 1500° F. Long-time tests were conducted at 1200° and 1350° F. Increasing the temperature from 1200° to 1350° F reduced the expected operating life by at least a factor of 25.

The physical strengths of the fir-tree designs depended solely on the cross-sectional areas carrying the tensile and shear loads, whether provided by a few large serration teeth or many small teeth. The root strengths correlated well with physical properties of the blade and wheel materials as determined by simple tensile, stress-to-rupture, and 1/8-inch-diameter-pin long- and short-time shear tests.

INTRODUCTION

In the aircraft gas-turbine field, almost all turbine blades made from conventional heat-resisting materials are held in the rotor rim by some form of serrated fir-tree root. However, large variations exist in the shape, size, and number of serrations from one design to the next. Apparently, there is a wide difference of opinion concerning the best serration design. Very little literature is available on the design of roots, and the information that does exist is usually of a proprietary nature.

The NACA, therefore, after a preliminary survey of the inherent advantages of various blade roots, undertook an investigation of the important factors affecting the strength of the fir-tree root form. In order to explore the problems encountered with typical blade roots, three specific production root designs were investigated. Test specimens fabricated with the three serrated-root profiles were subjected to various loads and temperatures until rupture occurred, and these results are

correlated with the mechanical properties of the materials involved. The effect of blade vibration is not included in this work, because vibrations differ widely from engine to engine and measurement of vibration amplitudes in service is very difficult. Furthermore, it is impossible to predict the magnitude of vibratory stresses that will exist in a new engine. Also, bending stresses due to blade tilt and gas forces were not considered in this report, because by careful design of the airfoil these two effects can be counterbalanced. Bending stress in blade roots were extensively investigated in reference 1 in connection with cermet blades, where bending stresses are very important.

APPARATUS, MATERIALS, AND PROCEDURE

Specimens of several different types were used in this investigation. The one used to the greatest extent is shown in figure 1. The root shapes were cut in the ends of long bars so as to remove the grips from the furnaces. The root ends were restricted to 1/4-inch thickness because of the limited load capacity of the stress-rupture machines. The three fir-tree root profiles investigated, which are specific designs actually used in service, are designated blades A, B, and C (fig. 2). The specimen components corresponding to the blade roots were cast from Stellite 21 rather than forged from S-816 or other current blade materials because of the relatively low cost of forming and the availability of the casting material. The component representing the turbine rotor segment was machined from Timken 16-25-6 alloy processed in the same manner as conventional disk forgings. The restraining fixture shown in figure 3 was assembled around the specimen to prevent the rotor component from spreading under load.

Another style specimen, shown in figure 4, was used to evaluate the strength of the turbine wheel segments between adjacent blades. The blade component was again cast from Stellite 21 but was made in two pieces to facilitate grinding of serrations. The parts representing wheel segments were actually machined from production turbine rotors. The same restraining clamps used with the other specimen were again used here.

In order to determine the mechanical properties of turbine blade and rotor materials, the notched and unnotched tensile specimens and the 1/8-inch-diameter shear-pin specimen shown in figures 5 to 7 were utilized. The testing was conducted in both screw and lever stress-rupture machines. Chromel-alumel thermocouples were placed in the locations where failure was expected.

Short-time tensile and shear tests were run at various temperatures ranging from room temperature to 1500° F. Most of the stress-rupture tests were conducted at 1200° F and a few were run at 1350° F. In all the elevated temperature tests, the temperature was permitted to stabilize for at least half an hour before the load was applied.

CALCULATION OF STRESSES

In order to determine the stresses resulting from tests of serrated specimens, some assumption must be made concerning the shear areas of the teeth. In determining the shear stresses, the question arises as to what cross-sectional area is actually subjected to the shearing action. From figure 8 it is apparent that two different extremes of the shear plane could be considered, as indicated by the two types of dashed lines. Both planes are parallel to the radial line passing through the center of gravity of the blade, which for the roots investigated was approximately coincident with the root center lines. One plane, however, is tangent to the apex radius of the serration tooth applying the load. This shear plane would probably be in effect just before ultimate failure occurred. The other plane contains the line where contact is terminated between the loaded and the loading tooth and should correspond to the shear plane acting when load is first applied before any deformation has taken place. For all computations of shear stress, the mean of these two shear areas was used, and it was further assumed that the shear stresses in all teeth were equal. The effective tensile area used in determining the tensile stresses was the minimum area across the serration fillets.

In order to predict the life and mode of failure of the different root components under the normal loads imposed by each specific engine on its corresponding root design, it is necessary to determine the loads and stresses imposed on these parts during rated engine speed and temperature. Table I presents this information for each of the three designs. The operating load at the top serration of the blade is based on the combined weight of the particular airfoil for which the root was designed, the platform, and that part of the root above the top serration. The shear load acting on the blade teeth is determined by considering the weight of the whole blade minus the projecting part of the teeth. The shear load acting on the rotor serrations is computed by adding the weight of the teeth on the rotor segment to the total blade weight. The tensile load on the turbine rotor segment includes the whole blade weight and the rotor segment beyond the neck of the bottom serration. From the table, it is apparent that the highest stresses occur in tension at the bottom rotor serration.

RESULTS AND DISCUSSION

Many methods and root variations have been introduced in the past for attaching turbine blades to the rotor. However, only the fir-tree forms have continued to be used extensively. In the appendix to this report, the merits of the four basic root profiles shown in figure 9 are compared and the reasons for the superiority of the fir-tree design are given. The more extensive investigations reported herein were therefore limited to variations of the fir-tree configuration.

Three specific root designs were tested, one with six pairs of small serrations, one with six pairs of larger serrations, and one with only three pairs of larger serrations. These profiles are not hypothetical designs but have been mass-produced and have experienced thousands of hours of service operation. They were chosen to explore the important criteria for designing serrated roots, to observe the modes of failure, and to investigate the factors affecting the root strengths. The operating loads and stresses to which the root strengths are compared are based on the airfoil weight, rotor diameters, and rated speed of the particular engine for which the root was designed.

Short-Time Tests at Various Temperatures

First, a series of specimens of the type shown in figure 1 were pulled to destruction in relatively short times at different temperatures. Only specimens of blades A and B were tested, because those of blade C were not available at the time of the short-time testing, and the limited number of specimens received later were reserved for more important tests to be discussed later.

The mechanism of failure changed according to temperature and root proportions, as illustrated in figure 10. With blade A the failure was one of tension below 1200° F and shifted to a shear failure above 1200° F. Blade B failed in shear over the whole temperature range, with a single tensile failure occurring at room temperature. In order to explain the shift in failure mechanism, short-time test data for both mechanisms of failure were plotted against temperature for the materials involved (fig. 11). Tensile data were taken from the literature (refs. 2 to 4) and confirmed by NACA data from the unnotched tensile bar (fig. 6). Shear data were obtained by shearing 1/8-inch-diameter pins (fig. 7).

The data presented in figure 11 for tension and shear of the blade and rotor materials are converted to load per inch rim thickness for all three root configurations in figure 12. The reason for the shift in failure mechanisms is readily apparent in this figure. For blade A (fig. 12(a)), the strength is lowest across the tensile area of the blade root below 1400° F. Above 1000° F the shear strength of the rotor material drops more rapidly than the tensile strength of the blade as the temperature is increased; and, consequently, above 1400° F the strength is lowest at the shear area of the serrations in the turbine rotor. In tensile tests of root specimens, the transition in failure mechanism took place at 1200° rather than 1400° F. The reason for this discrepancy between experimentally determined material properties and root specimens is not known. Figure 12(b) shows the lowest strength existing in shear of the rotor segments throughout the entire temperature range. The proximity of the tensile strength in the blade to the rotor shear strength at room temperature accounts for the tensile failure at room temperature. As in

figure 12(a), shear strengths of the specimens in figure 12(b) are again slightly below the shear strength of the material. At first examination, it might be concluded that the assumed shear area is in error, but the excellent correlation between the long-time specimen strength and material shear strength based on the same assumed areas indicates that some other factor is responsible for lower shear strengths in the root than predicted by material data. This discrepancy may be caused by the lack of perfect matching between wheel and blade root teeth due to machining tolerances. At the higher temperatures, some plastic flow and creep take place, which load the teeth equally and possibly account for the better correlation between specimen and material properties above 1100° F and in the long-time tests.

Although short-time tests on the root of blade C were not actually conducted, converting the material properties of figure 11 indicates that a shift in type of failure can also be expected here (fig. 12(c)). Below 1250° F the fastening should fail in tension of the blade root; above 1250° F tensile failures of the rotor segments generally are to be expected.

When the root specimens are subjected to a tensile load as used in the test machines, the results will correlate with figure 12. When a blade is in a centrifugal field as in the case in an actual engine, however, a correction should be applied. The rotor must carry the whole blade and, in addition, must carry the rim weight in the centrifugal field. Likewise, the rotor serrations in shear must support their own weight as well as the centrifugal load of the whole blade; and the blade serrations must carry, in addition to the airfoil, the root weight below the top serration neck minus the blade serration weight beyond the shear plane. Computed correction factors are presented in table II. These correction factors were applied to (divided into) the data of figure 12 to obtain figure 13. Thus, in an engine, blade A (fig. 13(a)) would again have a shift in failure mechanism, but the transition would be one from tension in the blade root to tension in the rotor root instead of shear of the rotor serrations. At 1200° F the failure might be either these types or shear of the rotor serrations, since all three lines intersect proximately.

In the engine, blade root B (fig. 13(b)) would probably again fail in shear of the rotor teeth throughout the temperature range, although above 1300° F the effective rotor strength in tension decreases to approximately the magnitude of the effective shear strength. Blade C in a centrifugal field should fail consistently in tension of the turbine rotor at all root temperatures below 1550° F, according to figure 13(c).

Besides the blade-strength correlations, other points of general interest can be deduced from the short-time data at different temperatures. For example, the shear strength cannot be assumed to be an

approximated constant ratio with respect to tensile strength as is the case for many materials at room temperature. The proportion, which varies from 50 to 100 percent, depends on both material and temperature (fig. 11). The rather surprising fact that the shear strength of Stellite 21 appears to be comparable in magnitude to the tensile strength (fig. 11(b)) was repeatedly checked with the same result. This result is probably explained by the relatively coarse grain structure of Stellite 21. Tensile failures are intercrystalline; but shear failures are generally transcrystalline, because the shear areas of the 1/8-inch-diameter pins and of the root serrations, carrying the shearing loads, are small and frequently confined within the grain. Evidently, the individual crystals or grains have shear strengths equal to the tensile strengths of the grain boundary material.

High-temperature alloy S-816 was also checked for shear strength (fig. 11(c)) and found to have very nearly the same short-time shear strength as Stellite 21. Thus, if the failure mechanism of a root is shear of the blade teeth, the results with S-816 should approximate those found with Stellite 21. If the failure occurs in tension of the blade root, an S-816 specimen would demonstrate higher strength than a Stellite 21 specimen.

Reasonably close agreement was obtained between shear properties of the materials as obtained by loading pins in double shear and the shear data of root specimens, particularly above 1200° F, the important range. There is some difference at lower temperatures probably caused by mismatching of serrations, but still the correlation is sufficiently close to justify the use of the material properties as determined from the simple pin in shear test as an approximate basis for root design.

Long-Time Stress-Rupture Tests at 1200° F

Short-time data are of limited interest in jet-engine design, because the turbine assembly must attain a reasonable operating life. In addition, low root temperatures are of little interest to the designer, because the fastening must be designed to withstand the maximum operating loads and temperatures.

The maximum rim temperature measured in reference 5 at rated speed was 1200° F. Therefore, a series of long-time tests at 1200° F was made with the three fir-tree root configurations. The results are presented in figure 14. Also included in the figure are operating stresses for the four critical regions of the fastening. The point of intersection of the horizontal operating-stress lines and the inclined lines through the stress-rupture data points indicates the maximum life expectancy at the rated-speed condition. Actual service life would be

three or four times this value, because only a small part of normal operating time is conducted at rated or take-off speed.

The mean life of blade A (fig. 14(a)) would be well over 2000 hours, and the failure mechanism should be one of shear of the turbine rotor serrations. Blade B (fig. 14(b)) has a much shorter life at rated speed, and the failure mechanism is again one of shearing of the rotor serrations. Blade C (fig. 14(c)) has a still shorter life, totaling 400 hours, but the rotor segment between blades should fail in tension across the bottom pair of serrations. Therefore, all failures of the roots investigated should occur in the rotor. In service, tensile failures occasionally occur in the blade root, whereas the data presented show a conservative safety factor in the blade root both in tension and shear. This discrepancy is logically explained by the presence of vibrations that cannot be predicted accurately.

Long-Time Tests at Increased Temperature

In the jet-engine industry attempts are constantly being made to increase turbine temperatures to obtain more thrust from the same engine. Therefore, the root-evaluation program was expanded to cover a temperature increase of 150° F (up to 1350° F). Only the turbine rotor strengths were determined, because the blade roots generally operate at lower stresses than the rotor and the blade materials have higher strength than the rotor materials at the increased temperature.

Turbine rotor A has sufficient strength at the higher temperature and could be used without alteration, provided the blade airfoil can either withstand the increased temperature or can be cooled by some method (fig. 15(a)). The life, however, is reduced from well over 2000 hours to 700 hours. Rotor B (fig. 15(b)) also would be suitable for limited life at the higher temperature, its life being reduced to 150 hours at rated-speed conditions. Blade root C (fig. 15(c)) would be applicable only for short life or for expendable missile service at 1350° F rim temperature without a major redesign. The mean life is 16 hours, compared with 400 hours at 1200° F rim temperature, or a ratio of 25:1. If a higher constant shear stress of 20,000 psi is assumed for both temperatures for blade roots A and B, so that extrapolation becomes unnecessary, the ratios of life for 1200° to 1350° F are 40:1 and 33:1, respectively. The mechanism of failure at 1350° F is still one of shear of the serrations for roots A and B and again one of tension across the rotor serrations for root C.

By replotting some of the data of figures 14 and 15 so as to compare like failure mechanisms for the three different roots, some interesting correlations are derived. In figures 16(a) and (b) the rupture data for the blade materials are compiled along with data from several references.

The casting alloy, Stellite 21, from which many of the root specimens were made, is apparently insensitive to notches with fillets down to 0.0135-inch radius (fig. 16(a)). The S-816, however, from the limited data obtained, is greatly affected (fig. 16(b)). Evidently, each turbine blade material must be independently evaluated to determine the proper mechanical properties to be used in root design.

For the rotor material, assuming the shear data as obtained from the simple pin test at both 1200° and 1350° F were sufficiently accurate to use for design basis, the shear areas chosen for computations are apparently correct, as indicated by the close agreement between pin and root shear data plotted in figure 16(c). Serration fillet radius had no effect on the shear properties, as indicated by the roots of different radii. The long-time tensile properties of the rotor material, however, are affected by fillet radius as shown in figures 16(d) and (e). The effect is more pronounced at 1200° than at 1350° F. The unnotched NACA tensile data for Timken 16-25-6 agree very well with the tensile data obtained from specimens cut from turbine disks (ref. 7).

REMARKS ON CRITERIA FOR FIR-TREE ROOT DESIGN

From the data presented, several conclusions can be drawn that should be helpful in the design of mechanical fastenings for turbine blades. The shear area as determined from the section on CALCULATION OF STRESSES appears to be suitable for design purposes, if it is assumed that the data determined from the simple pin in shear test are reasonably accurate for obtaining shear strengths for design when actual root models or specimens are not readily available. At elevated temperatures, the shear strength cannot be assumed as a constant ratio or percentage of the tensile strength as it frequently is at room temperature; it is dependent on both material and temperature. The shear strength is not affected by the presence or the size of the serration fillets. Unnotched tensile data, however, are inadequate for determining the tensile strength of either the blade or the rotor component of a mechanical blade fastening.

The blade roots of all three designs investigated were much stronger in stress-rupture than their corresponding rotor serrations. By reducing the blade root tensile and shear areas in order to permit increasing cross-sectional areas of the rotor segments, the net strength of the blade attachment could be greatly increased. If the two parts were ideally proportioned, both the blade and rotor roots would be stronger than necessary. Then the rim thickness could be reduced and the entire engine made considerably lighter.

Blade roots should be slightly less conservative than rotors, because a rotor failure means the loss of a far more costly component of the engine, and a rotor failure is usually far more devastating than a blade failure.

Bearing stresses at the contact surfaces should not be excessive but also should not be too low. With low bearing stresses, only part of the total number of serrations will carry the centrifugal load unless the tolerances are unreasonably narrow or unless considerable plastic flow of the teeth in tension or shear takes place. As a result, premature tensile or shear failure may occur. With higher bearing stresses, plastic flow and creep will take place at the high bearings spots where it is less detrimental, and the loads will become evenly distributed among all teeth.

Root strengths can be evaluated on the basis of the physical properties of the materials and the actual dimensions for all the designs tested. For example, shear strength of a design is determined by shear area and material strengths in shear, whether the shear area is provided by many small serrations or by a few large serrations. Therefore, with respect to economy of production, since strength is not sacrificed, the fewer number of large serrations result in the better root form. The larger teeth and fillets are also advantageous with respect to vibration. The fillet size had little effect on the tensile strength of the root but has a large effect on the distribution and concentration of stresses in the presence of vibration; and, consequently, it greatly affects the fatigue properties. A compromise in fillet size must be retained, because increased fillet radii tend to decrease the available areas supporting the shear load.

Bending stresses due to blade tilt and gas forces were not considered in this report, because by careful design of the airfoil these two effects can be counterbalanced. Bending stresses in the root can be further reduced by properly skewing the root axis with respect to the turbine axis to the best alinement with the airfoil position, as outlined in reference 1.

SUMMARY OF RESULTS

In order to explore the failure mode and the factors affecting root strength, short- and long-time rupture tests were conducted at various temperatures on three different fir-tree root designs from existing turbojet engines. The following results were obtained from analysis of the data:

1. The root strengths were dependent only on the total tensile and shear areas available to support the loads and were not directly affected by the number or size of the serrations providing these areas.

2. In the three configurations tested, ultimate failure, due to a simulated centrifugal load and temperature corresponding to normal operation of the engine for which the respective roots were designed, occurred in the rotor segment. The mechanism of failure was shear of the rotor teeth in two of the roots and tension across the lowest neck in the other case.

3. The ratio of the tensile strength to the shear strength at elevated temperature in the short-time tests varied from 2:1 to 1:1, depending on the material and temperature.

4. Also, the shear strength in stress-to-rupture is dependent on material, temperature, and time, and is not a constant proportion of the tensile strength in stress-to-rupture.

5. Increasing the test temperature 150° F from 1200° to 1350° F reduced the life of the root fastenings by a minimum factor of 25.

Lewis Flight Propulsion Laboratory
National Advisory Committee for Aeronautics
Cleveland, Ohio, June 3, 1954

APPENDIX - ROOT PROFILES

Many root forms have been proposed for fastening turbine blades to the rotor. In figure 9 are illustrated a few of the more important basic configurations, of which variations have been introduced in recent years. The percentages listed under each root type indicate the amount of the maximum available tensile or shear area that was actually utilized by each type. A 100-percent tensile area of the blade root, for example, would mean that the root neck of the blade touches those of adjacent blades and no space is left for the wheel segment. Thus, 100-percent tensile area is possible only if the blade is integral with the wheel or welded to it. The percentage shear area is obtained by dividing the actual area of the blade or the wheel segment supporting the centrifugal load in shear by the rim thickness multiplied by twice (double shear) the radial penetration depth for the fir-tree root d. The depth of fir-tree root was chosen so as to obtain a common basis for comparison. The actual numerical values, of course, can be varied considerably by adjusting the proportions of each design. Considerable discretion was involved in deciding the proportions to be used; all factors must be taken into account, including bearing loads, wheel strength, and so forth. The percentages calculated are reasonably representative of the highest values obtainable for practical configurations. The blade tensile area generally can be increased at the expense of either the shear area or the tensile area of the wheel, and vice versa.

By comparing percentage values it can be observed that the ball root has the highest shear values, but low tensile values. In fact, the fir-tree configuration has tensile values almost twice those of the other roots; and it is, therefore, appreciably more efficient than all the other forms. It is for this reason that only the fir-tree-root form has been used extensively for aircraft gas turbines, although many other roots have been tested.

The fir tree has the highest percentage tensile area without loss in shear area, as a direct result of its multiland construction. The tensile areas are large where the greatest tensile loads are applied. The number of serrations can be reduced while still retaining this advantage up to the point where only a single pair of serrations remain and the fir-tree root is essentially reduced to the form of the other roots shown in figure 9. Because the fir tree is apparently the strongest root for ductile materials, this report concentrates on determining design criteria for the fir-tree serrations.

REFERENCES

1. Meyer, A. J., Jr., Deutsch, G. C., and Morgan, W. C.: Preliminary Investigation of Several Root Designs for Cermet Turbine Blades in Turbojet Engine. II - Root Design Alterations. NACA RM E53G02, 1953.

2. Clark, F. H.: Metals at High Temperatures. Reinhold Pub. Co., 1950.

3. Anon.: Haynes Alloys for High-Temperature Service. Haynes Stellite Co. (Kokomo, Ind.), 1948.

4. Anon.: Technical Data on Allegheny Ludlum Alloy S-816. Allegheny Ludlum Steel Corp., Watervliet (N. Y.), Jan. 3, 1950.

5. Farmer, J. Elmo, Millenson, M. B., and Manson, S. S.: Study of Stress States in Gas-Turbine Disk as Determined from Measured Operating-Temperature Distributions. NACA RM E8C16, 1948.

6. Clark, C. L., Fleischmann, M., and Freeman, J. W.: Influence of Extended Time on Creep and Rupture Strength of 16-25-6 Alloy. Preprint No. 16, A.S.M., 1951.

7. Freeman, J. W., Reynolds, E. E., and White, A. E.: A Metallurgical Investigation of Five Forged Gas-Turbine Discs of Timken Alloy. NACA TN 1531, 1948.

8. Freeman, J. W., Rote, F. B., and White, A. E.: High Temperature Characteristics of 17 Alloys at 1200° and 1350° F. NACA WR W-93, 1944. (Supersedes NACA ACR 4C22.)

TABLE I. - LOADS, AREAS, AND STRESSES OF FIR-TREE ROOT FORMS INVESTIGATED

Root	Operating loads, lb				Load-carrying area, sq in.				Stresses at rated speed, psi				Rated engine speed, rpm
	Tension at blade top serration	Shear, blade	Tension at rotor bottom serration	Shear, rotor	Tension at blade top serration	Shear, blade	Tension at rotor bottom serration	Shear, rotor	Tension at blade top serration neck	Shear, blade	Tension at rotor bottom serration neck	Shear, rotor	
A	6,870	8,810	11,080	9,150	0.540	0.782	0.689	0.782	12,710	11,270	16,080	11,700	7,900
B	13,250	15,320	17,710	15,860	.909	1.002	.850	1.002	14,570	15,290	20,840	15,830	7,953
C	20,750	28,310	36,870	29,800	1.335	2.024	1.180	1.831	15,540	13,990	31,250	16,270	11,750

TABLE II. - LOAD-CORRECTION FACTORS

Blade	Tension, blade	Shear, blade	Tension, rotor	Shear, rotor
A	1.0	1.283	1.613	1.332
B	1.0	1.157	1.337	1.197
C	1.0	1.365	1.777	1.436

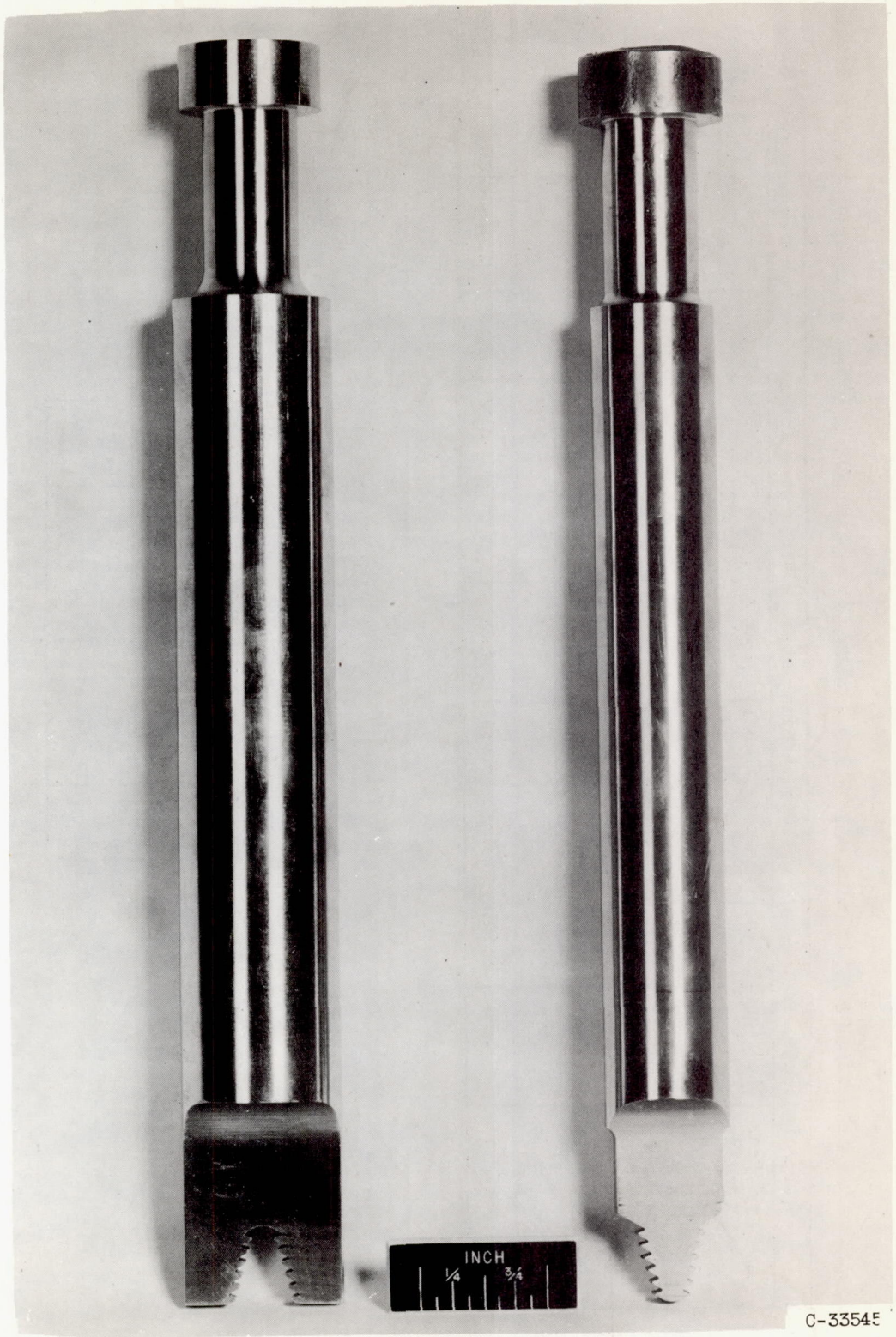

Figure 1. - Tensile specimen used to simulate turbine blade root.

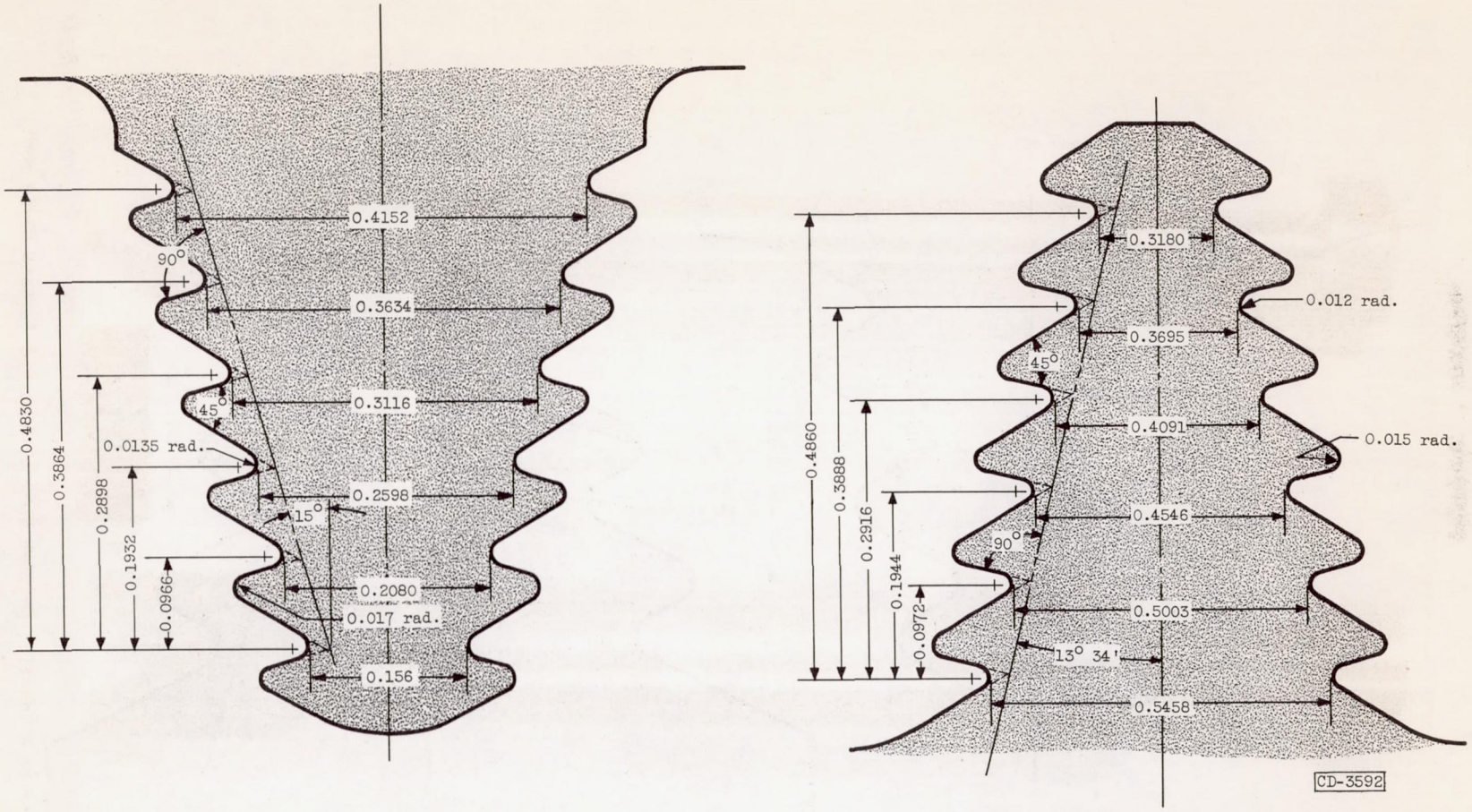

(a) Blade root A.

(b) Turbine rotor segment A.

Figure 2. - Dimensions of three fir-tree roots tested (inches).

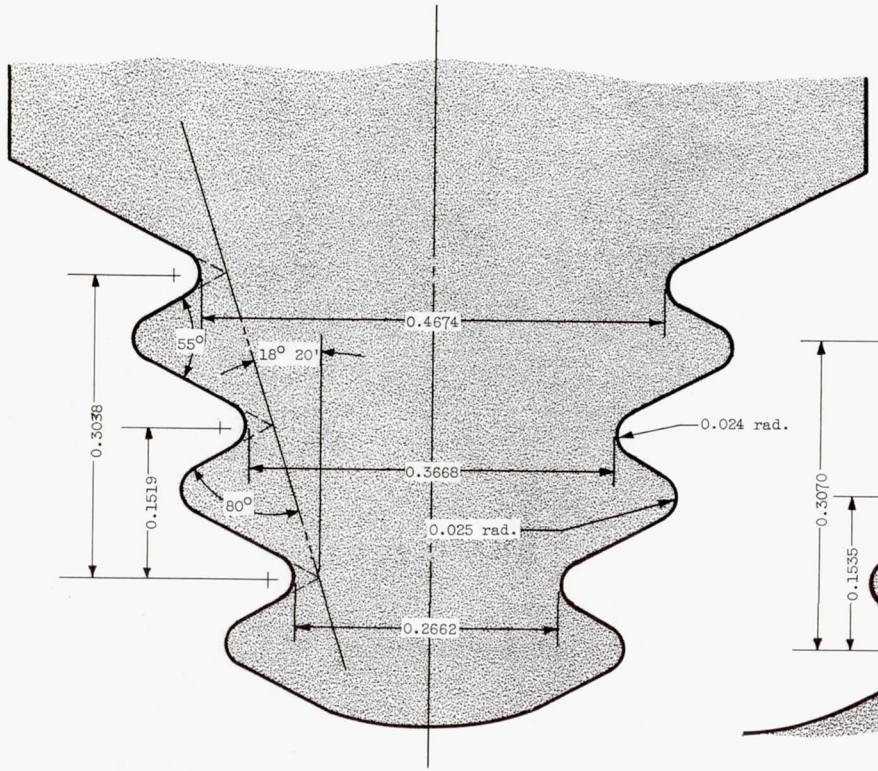

(c) Blade root B.

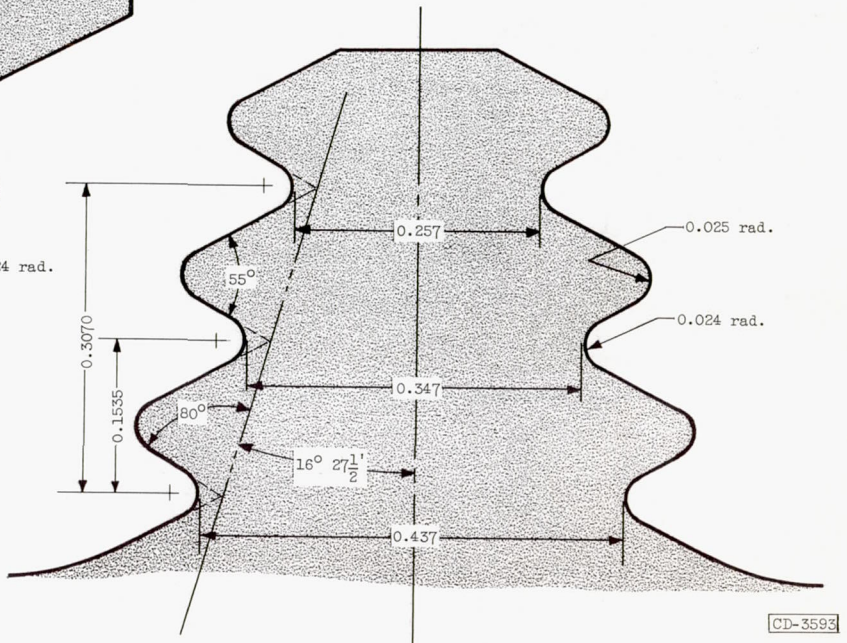

(d) Turbine rotor segment B.

Figure 2. - Continued. Dimensions of three fir-tree roots tested (inches).

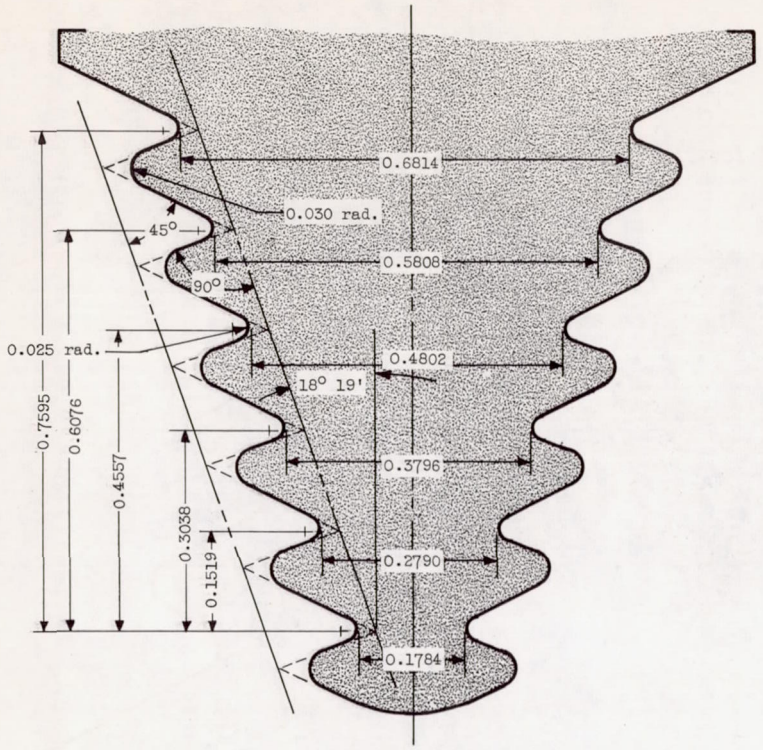

(e) Blade root C.

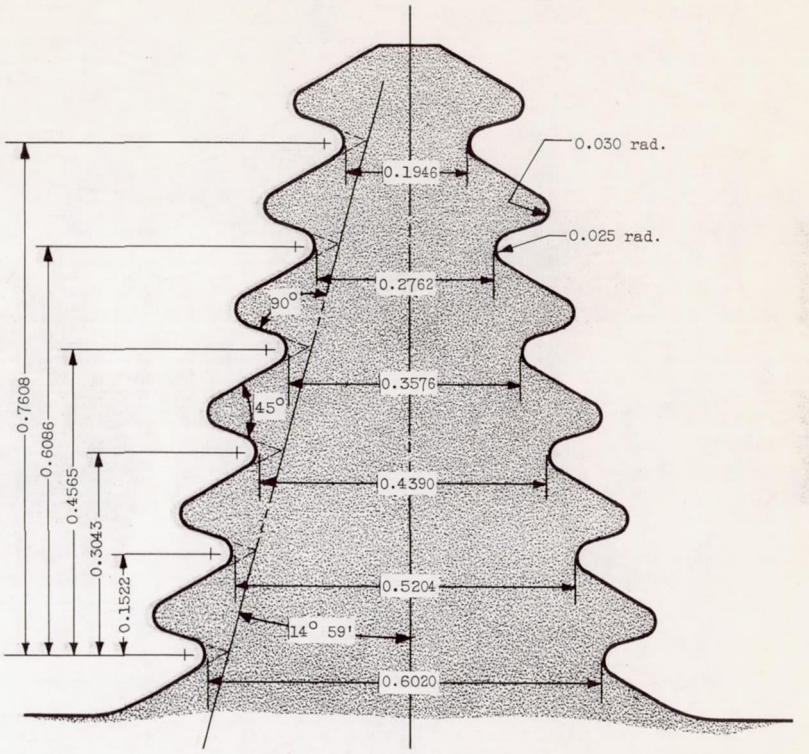

(f) Turbine rotor segment C.

CD-3594

Figure 2. - Concluded. Dimensions of three fir-tree roots tested (inches).

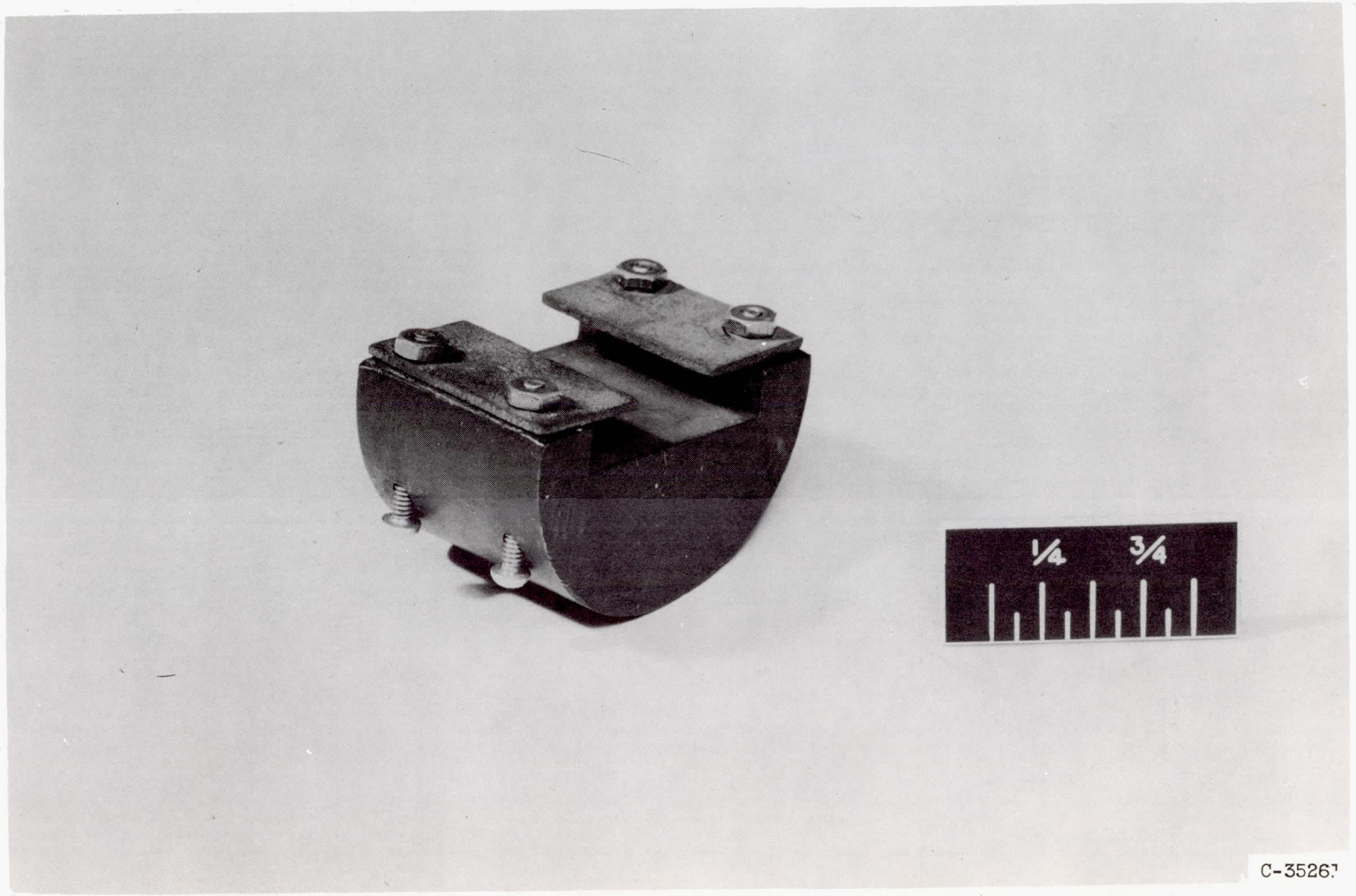

Figure 3. - Restraining fixture used in conjunction with specimens shown in figures 1 and 4.

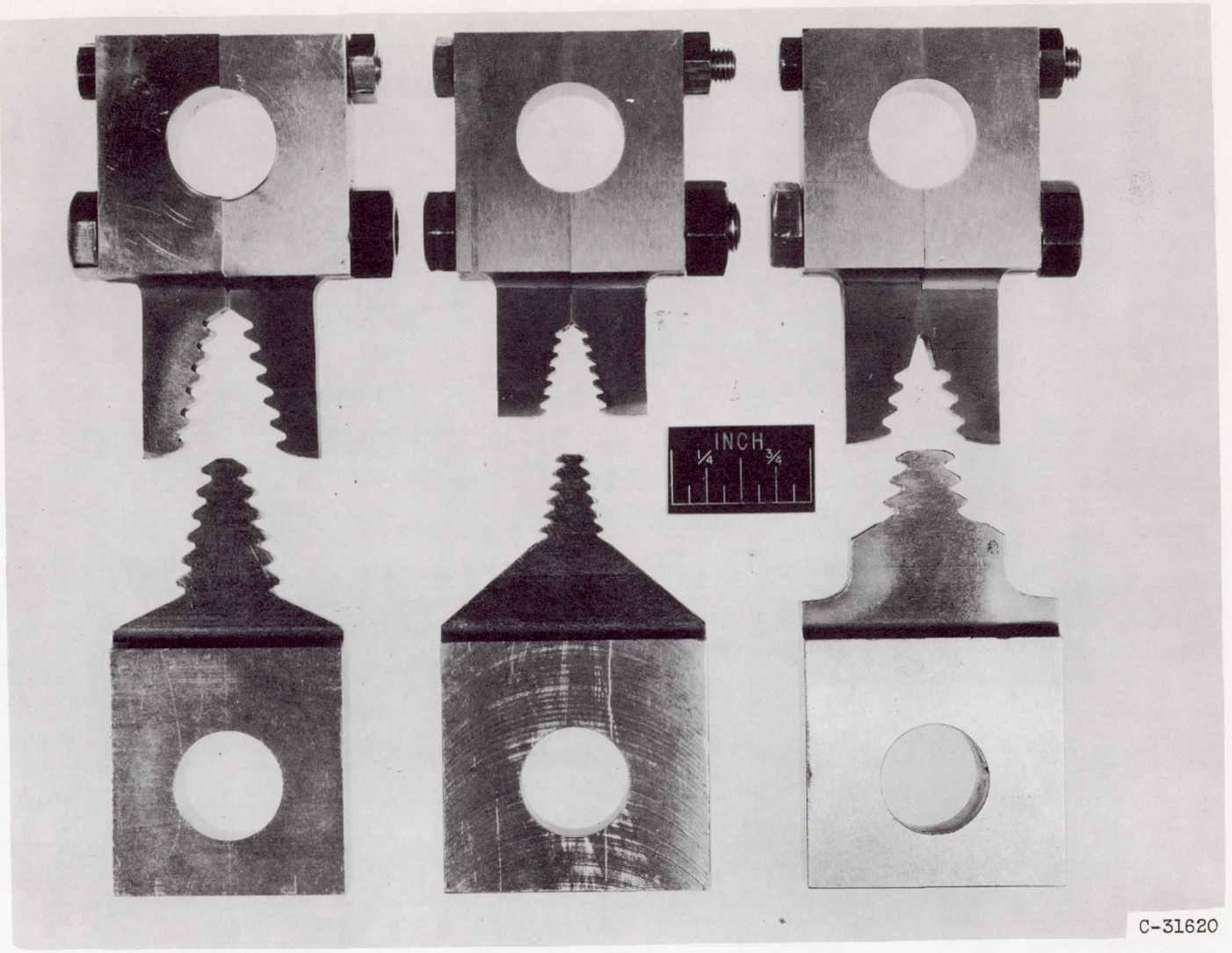

Figure 4. - Tensile specimens used to simulate turbine rotor segment between adjacent blades.

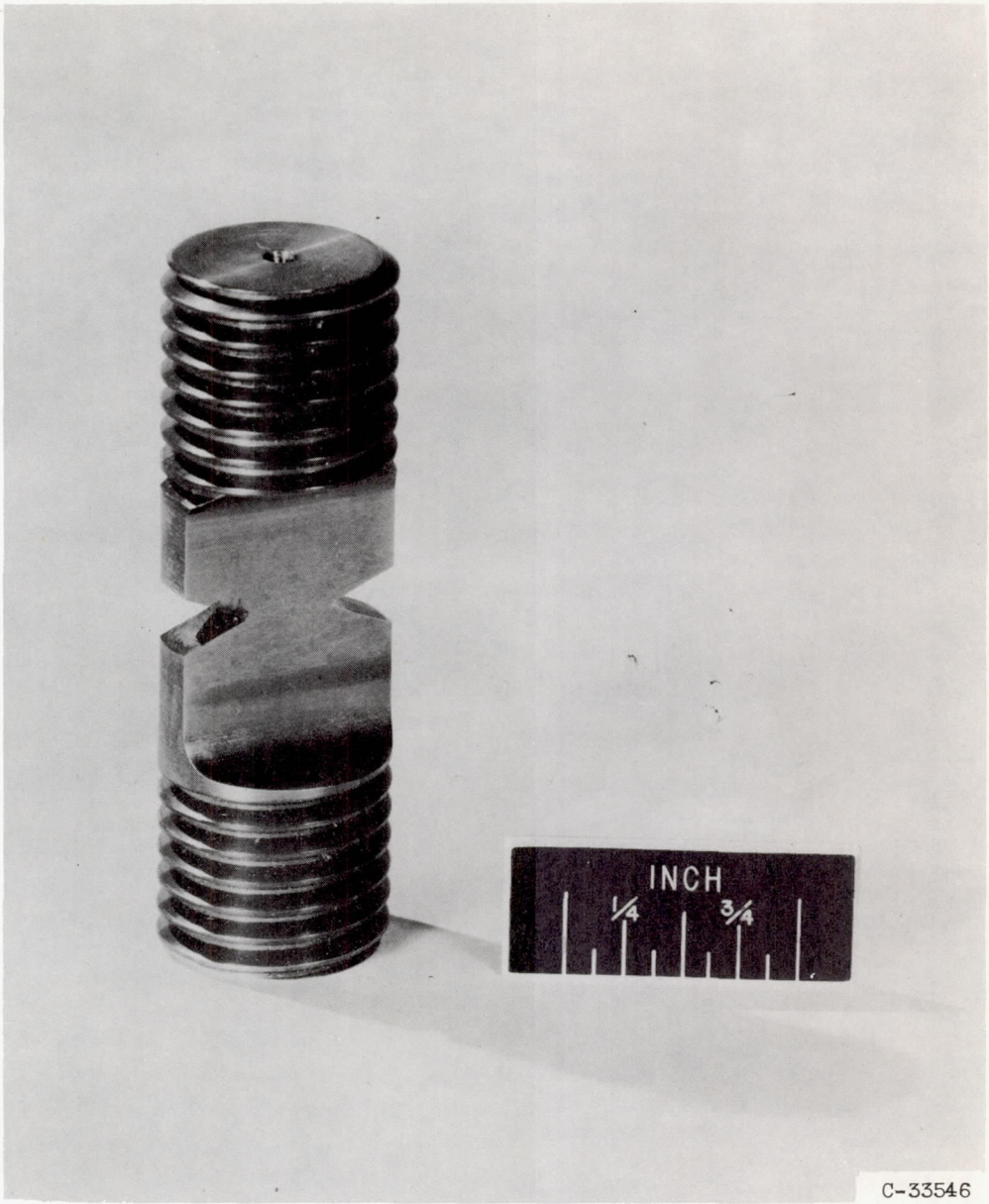

Figure 5. - Notched tensile specimen for determining material properties.

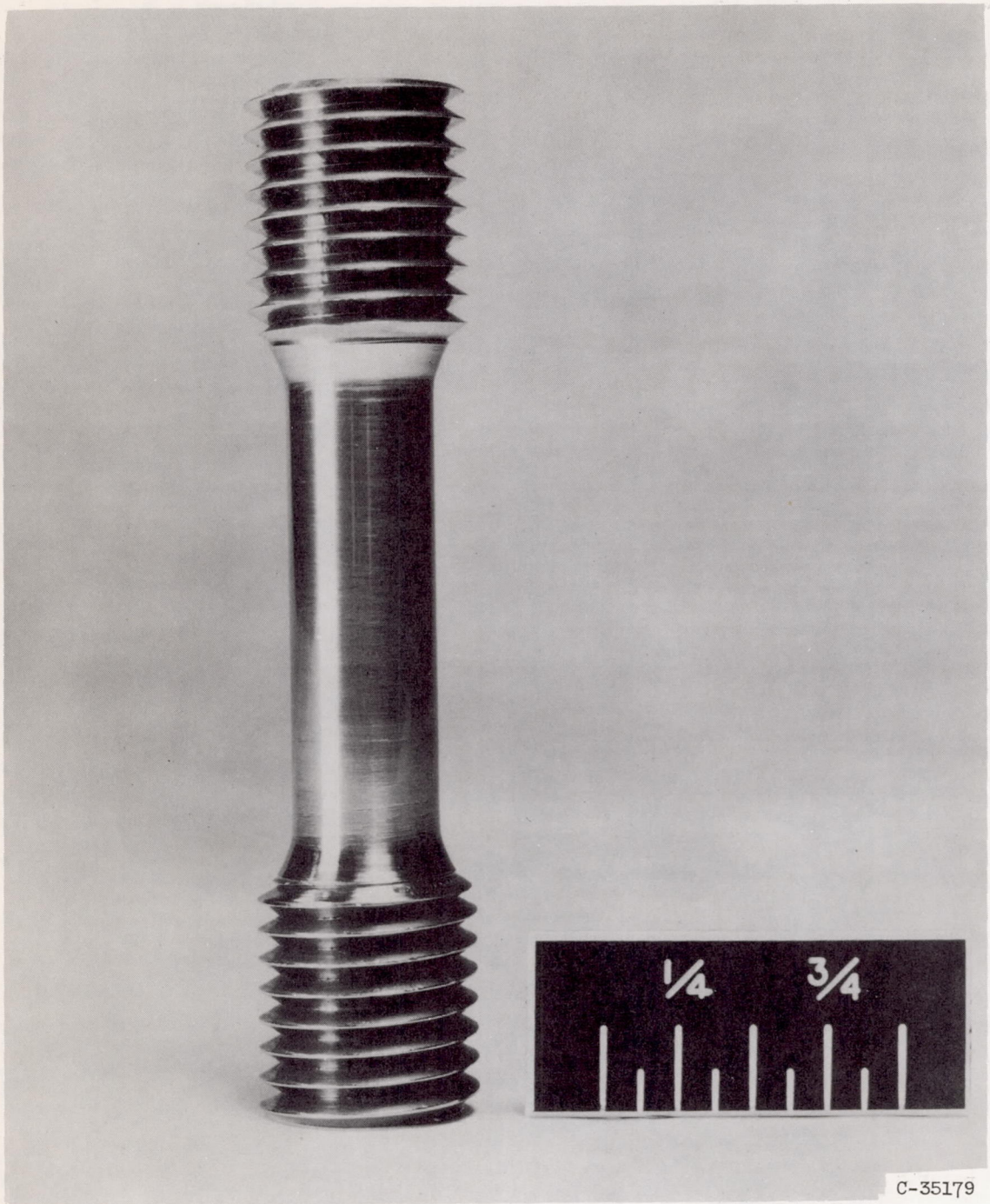

Figure 6. - Unnotched test bar for determining tensile properties of rotor material.

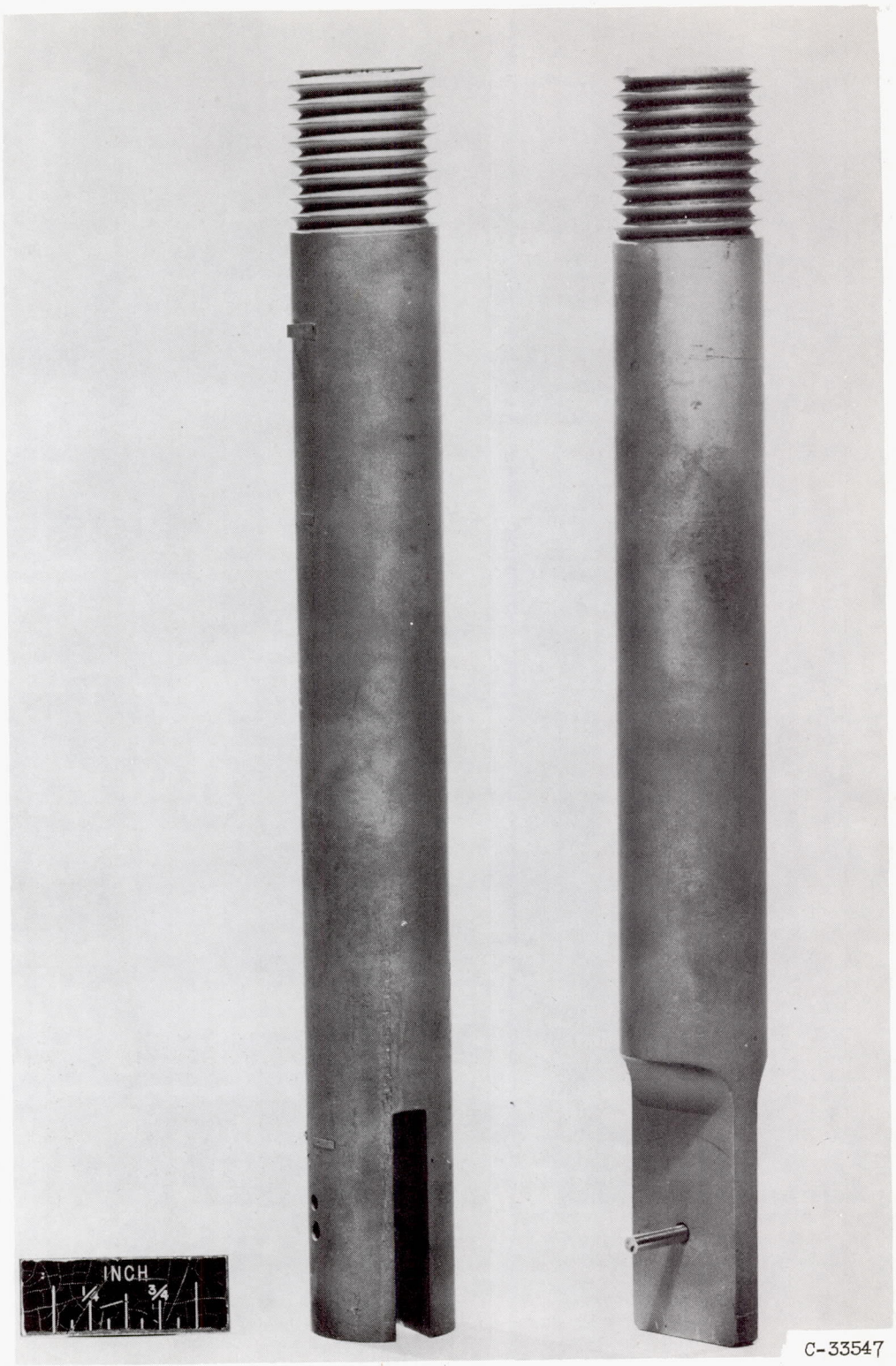

Figure 7. - Specimen and loading fixture for determining shear strength materials used.

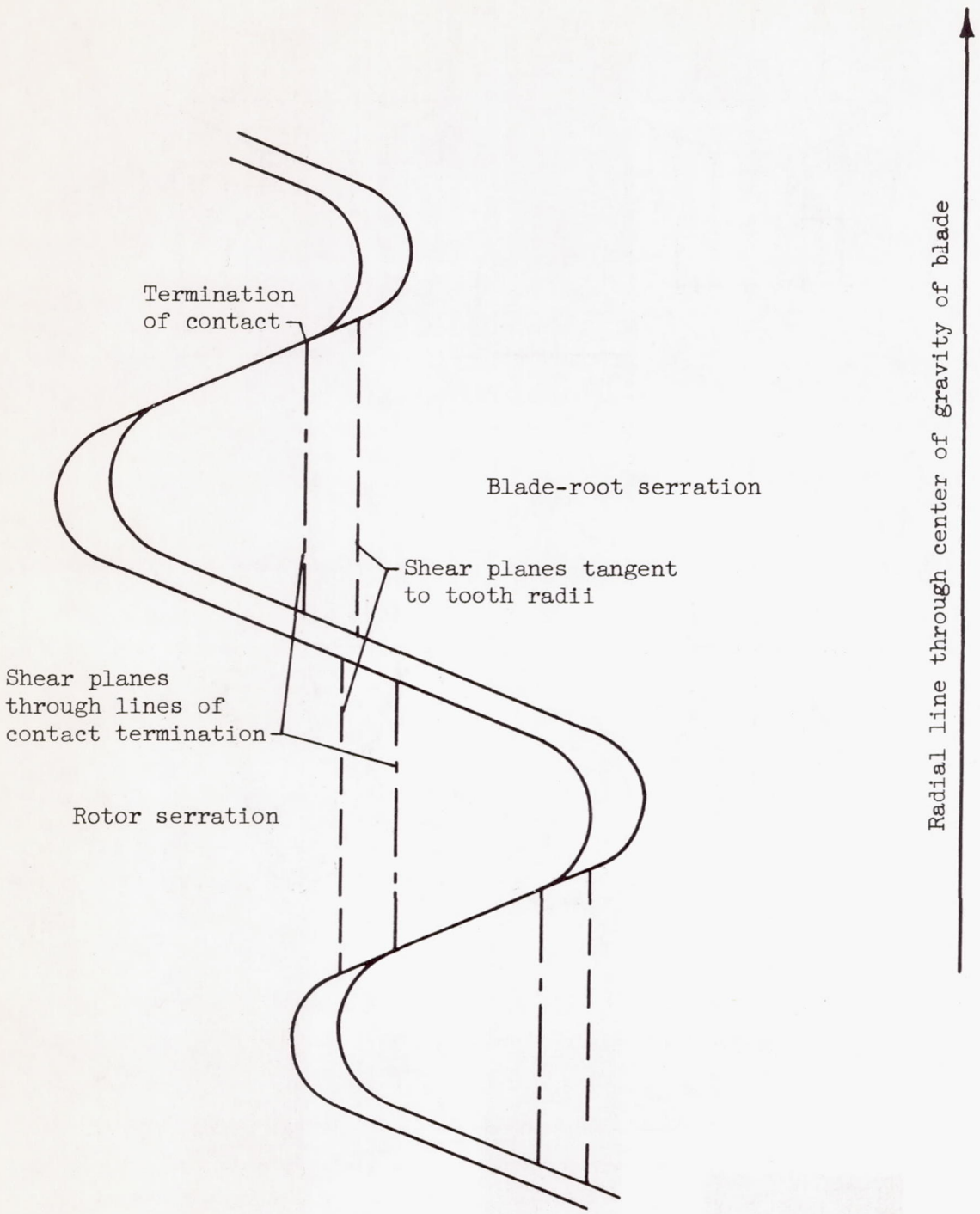

Figure 8. - Shear-plane locations used in computing shear stresses.

T root

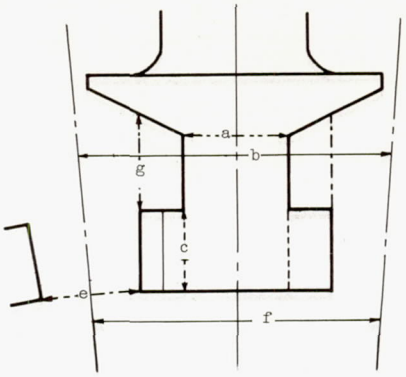

Ball root

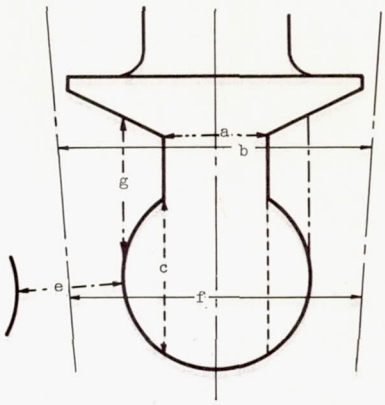

Blade	Tension, a/b	33 %	33 %
	Shear, c/d	29 %	53 %
Rotor	Tension, e/f	35 %	37 %
	Shear, g/d	35 %	53 %

Wedge root

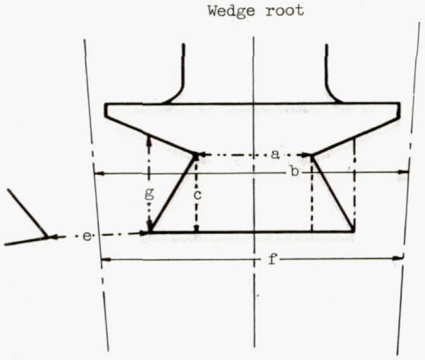

Fir-tree root

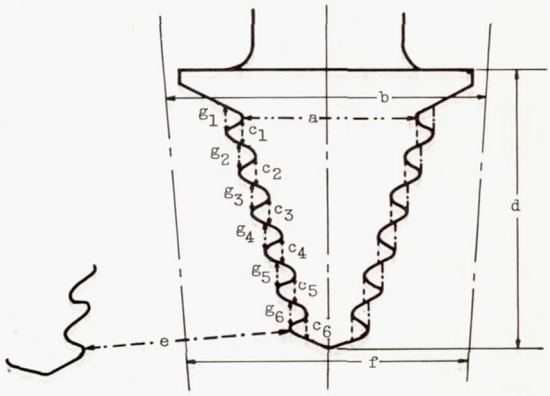

CD-3650

Blade	Tension, a/b	37 %	66 %
	Shear, c/d	33 %	49 % $(c_1 + c_2 + \ldots . c_6)/d$
Rotor	Tension, e/f	33 %	64 %
	Shear, g/d	38 %	49 % $(g_1 + g_2 + \ldots . g_6)/d$

a —··—·—··— Blade root tension plane

e —·—·—·— Wheel segment tension plane

c - - - - - - - - - - - Blade root shear plane

g —·—·—·—·— Wheel segment shear plane

b Blade spacing at platform

d Penetration depth of fir-tree root

f Blade spacing at root

Figure 9. - Basic root configurations.

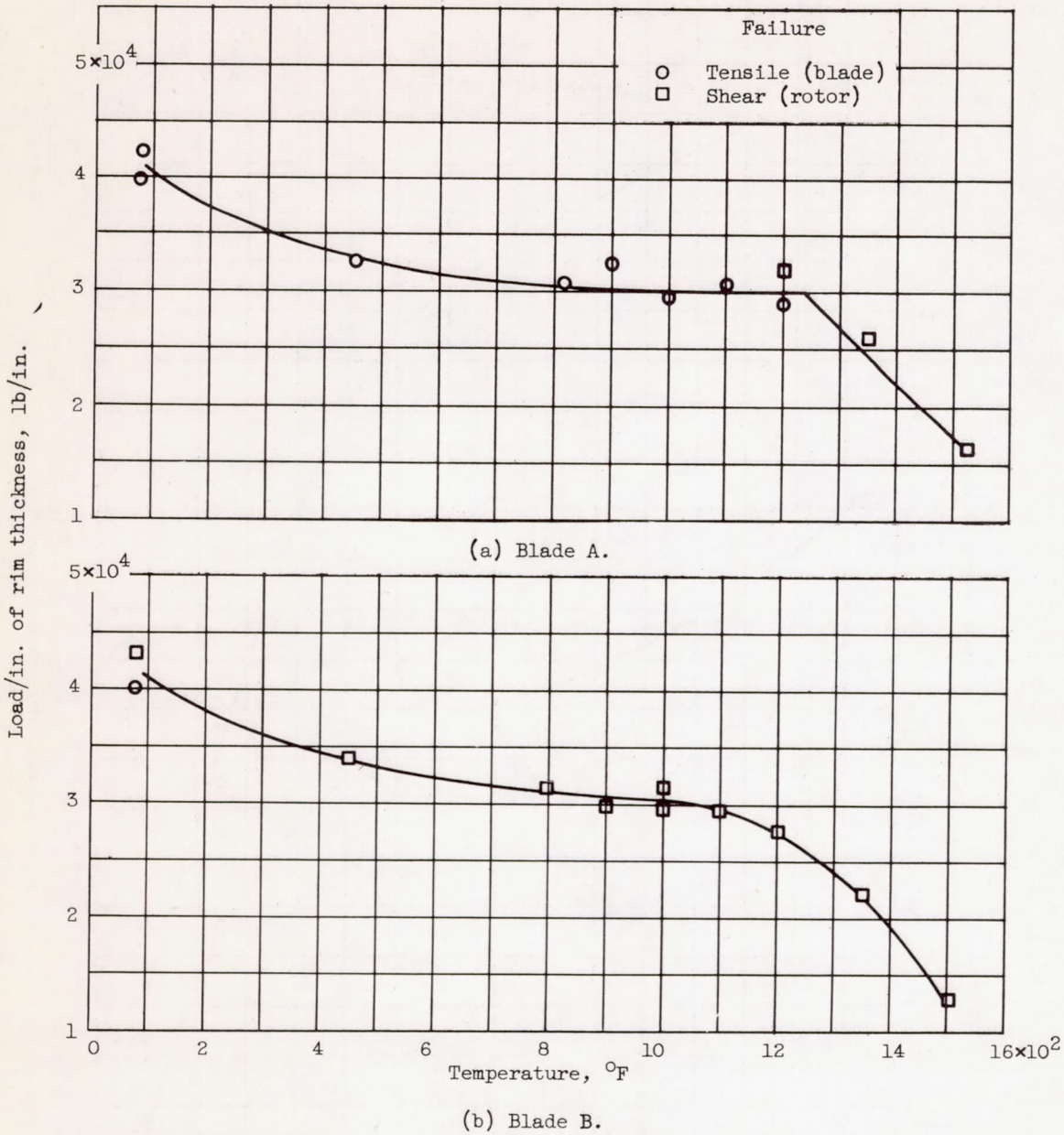

Figure 10. - Short-time tensile-test results at various temperatures for blade A and B specimens.

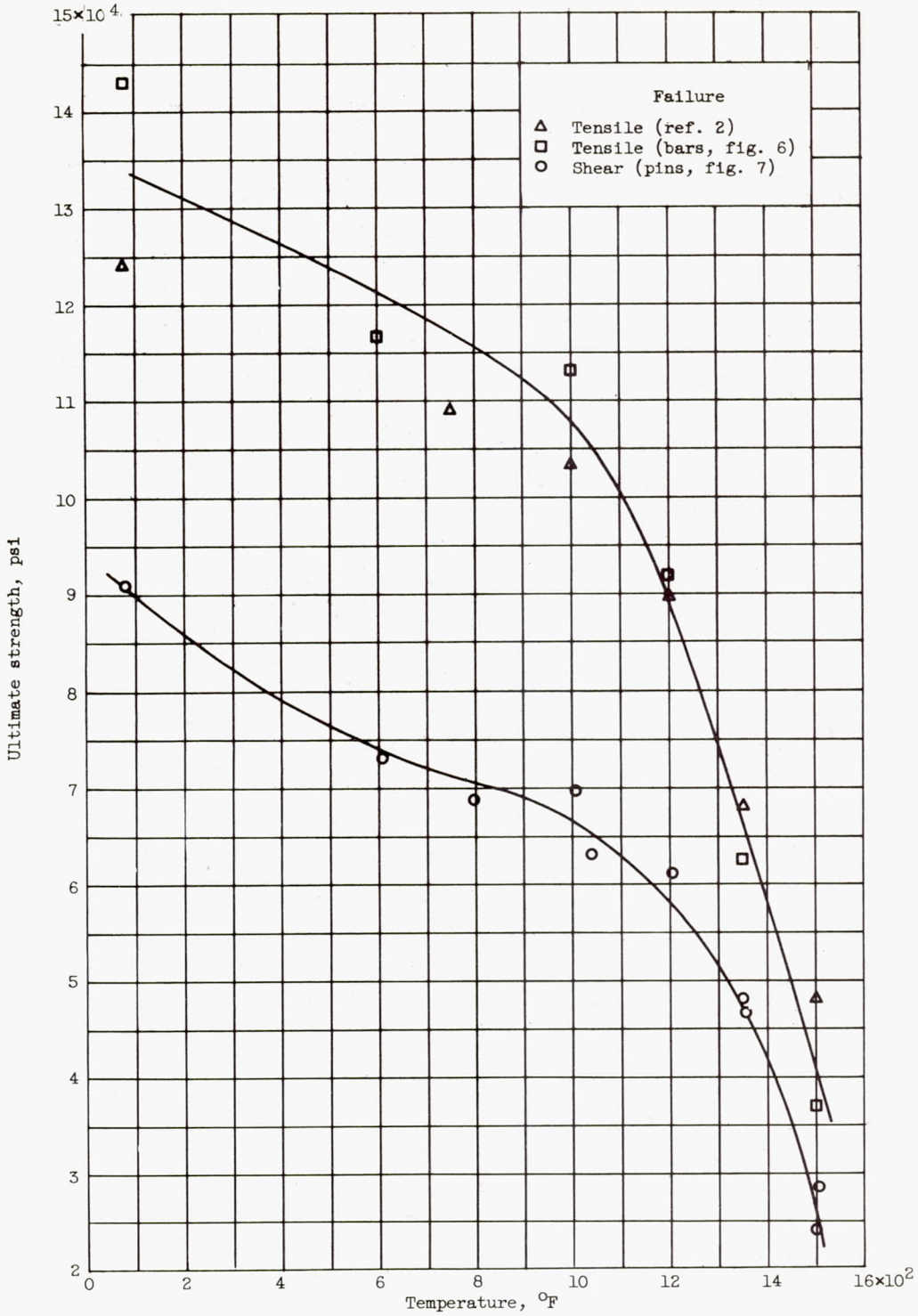

(a) Timken 16-25-6.

Figure 11. - Short-time tensile and shear properties of turbine blade and rotor materials at various temperatures.

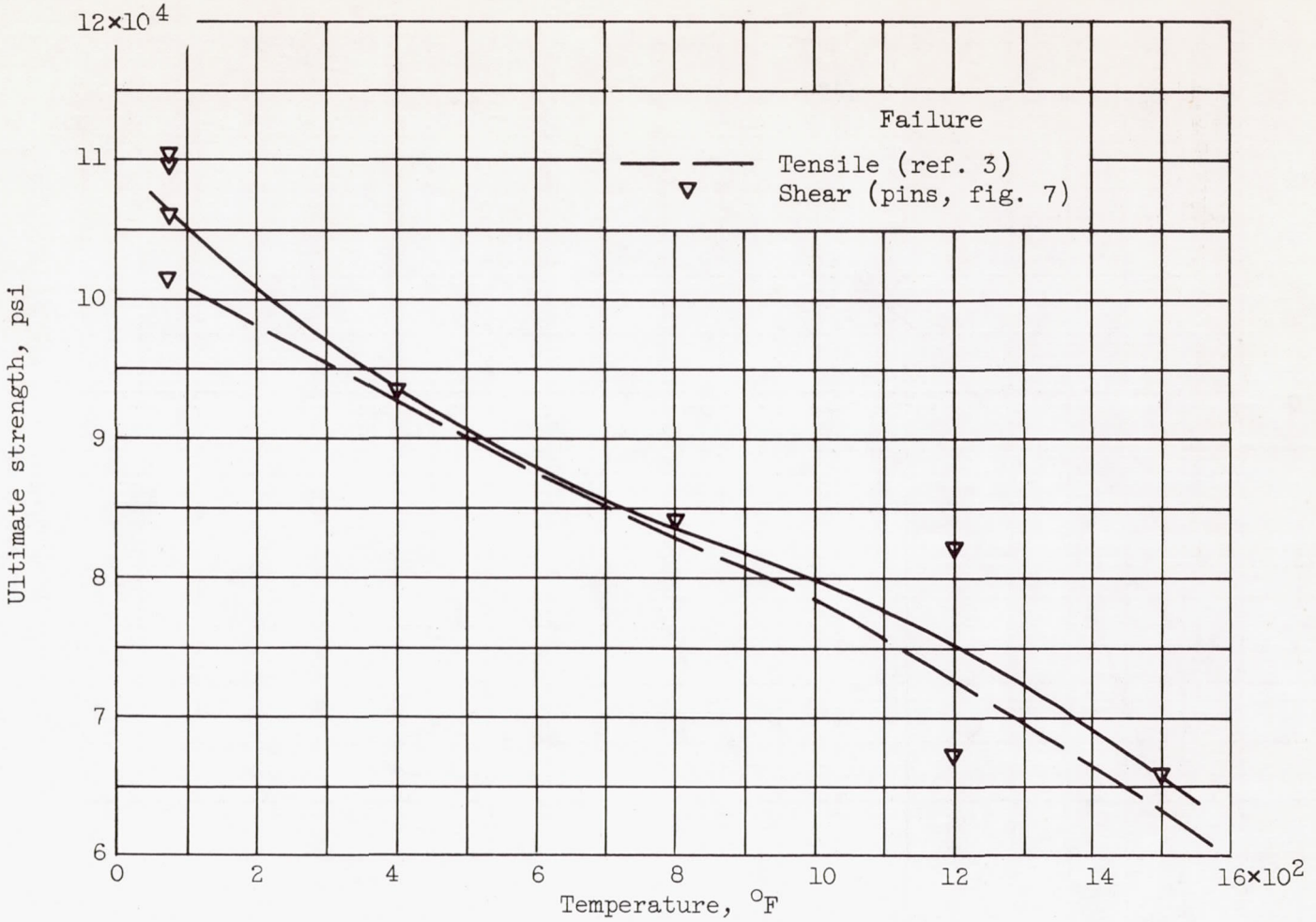

(b) Stellite 21.

Figure 11. - Continued. Short-time tensile and shear properties of turbine blade and rotor materials at various temperatures.

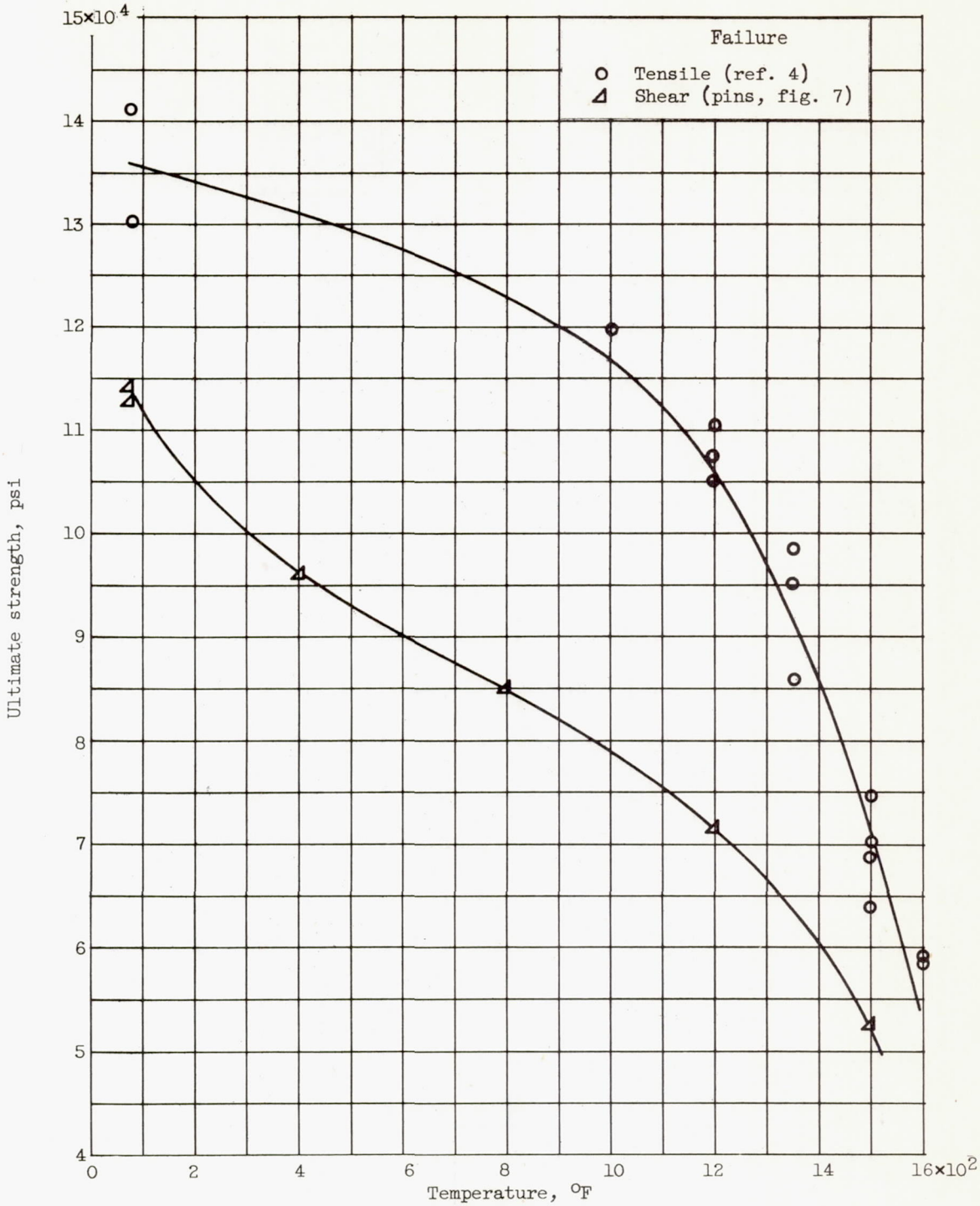

(c) S-816.

Figure 11. - Concluded. Short-time tensile and shear properties of turbine blade and rotor materials at various temperatures.

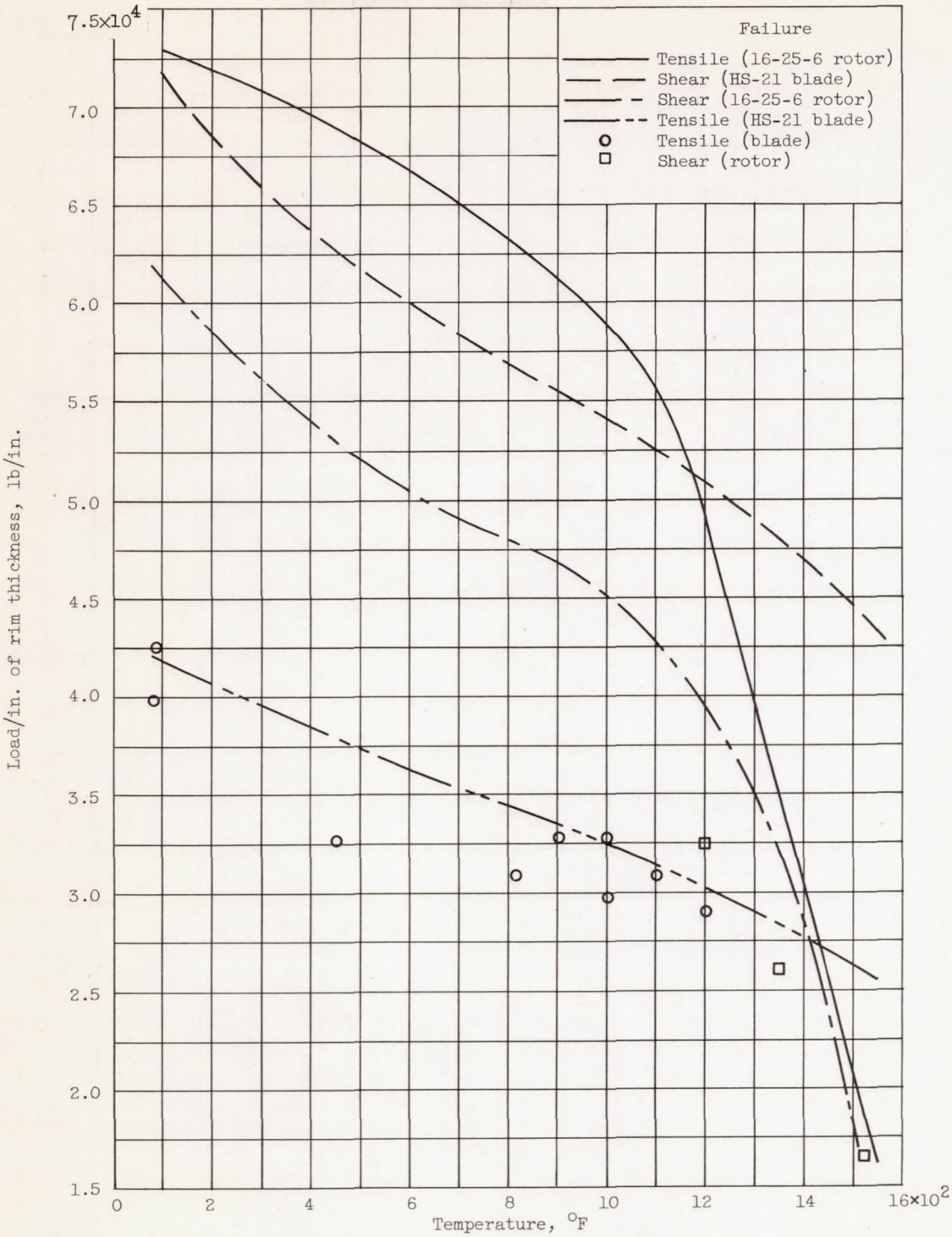

(a) Blade root A.

Figure 12. - Mechanism of short-time failure as result of variations in temperature.

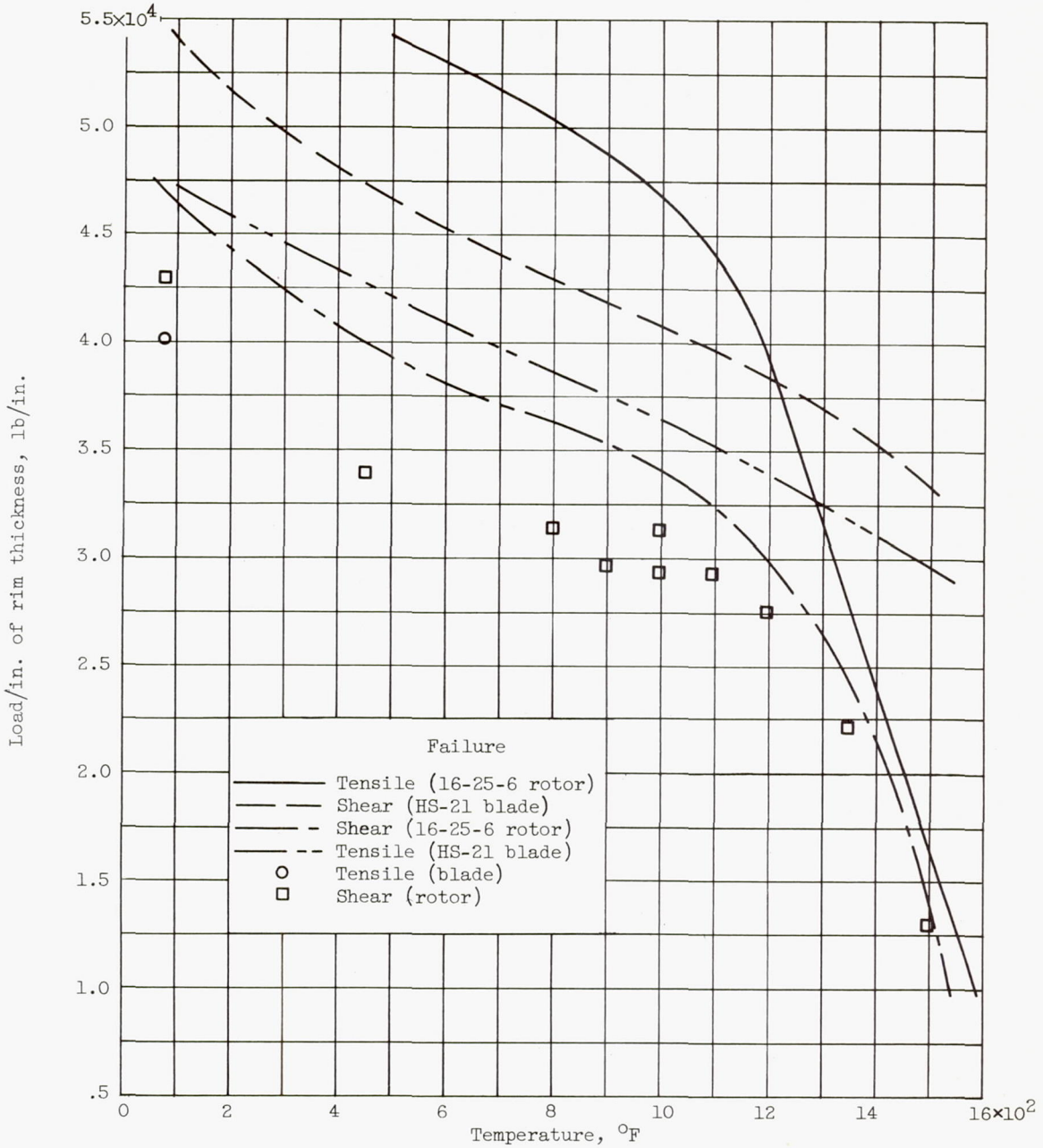

(b) Blade root B.

Figure 12. - Continued. Mechanism of short-time failure as result of variations in temperature.

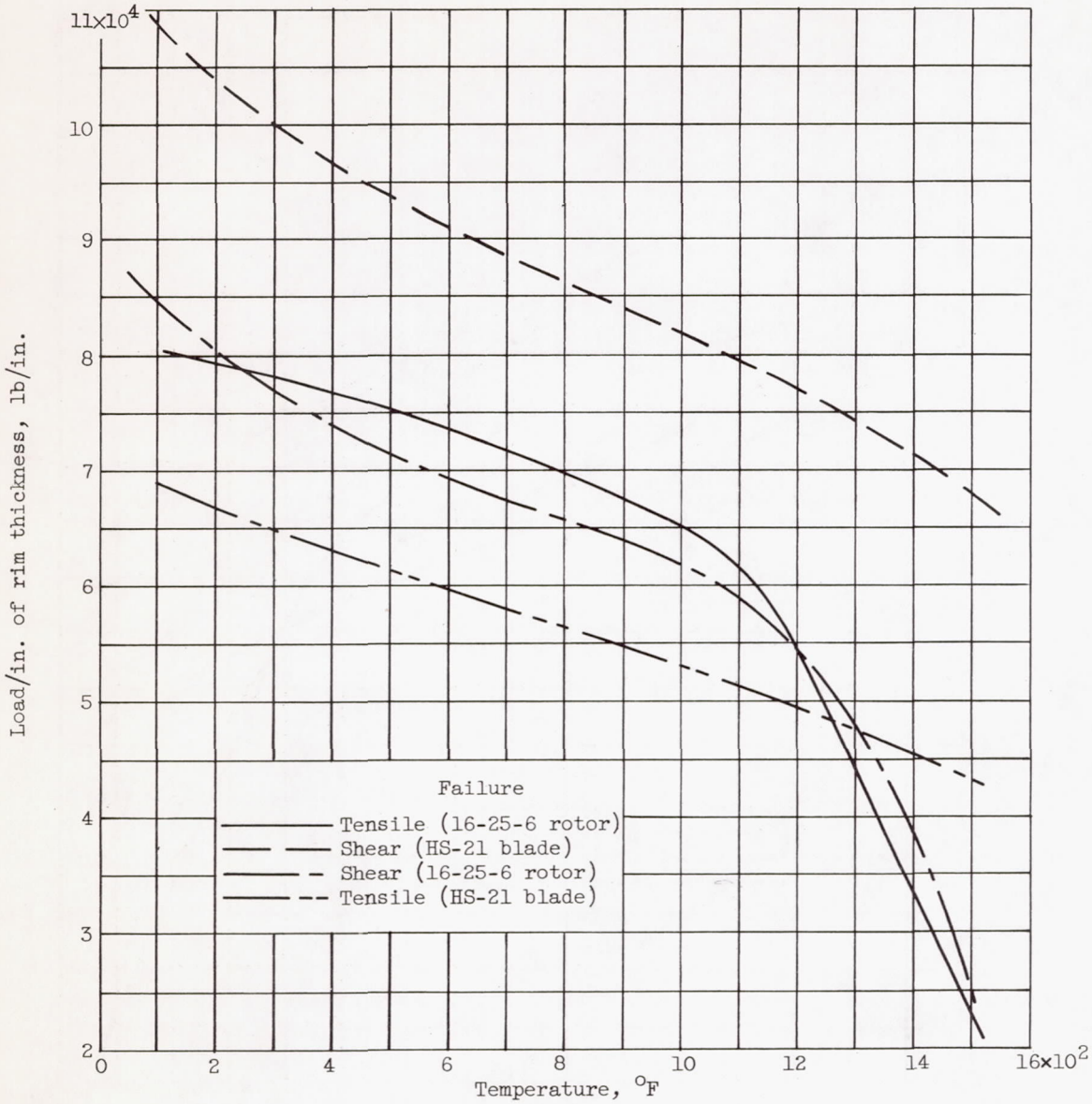

(c) Blade root C.

Figure 12. - Concluded. Mechanism of short-time failure as result of variations in temperature.

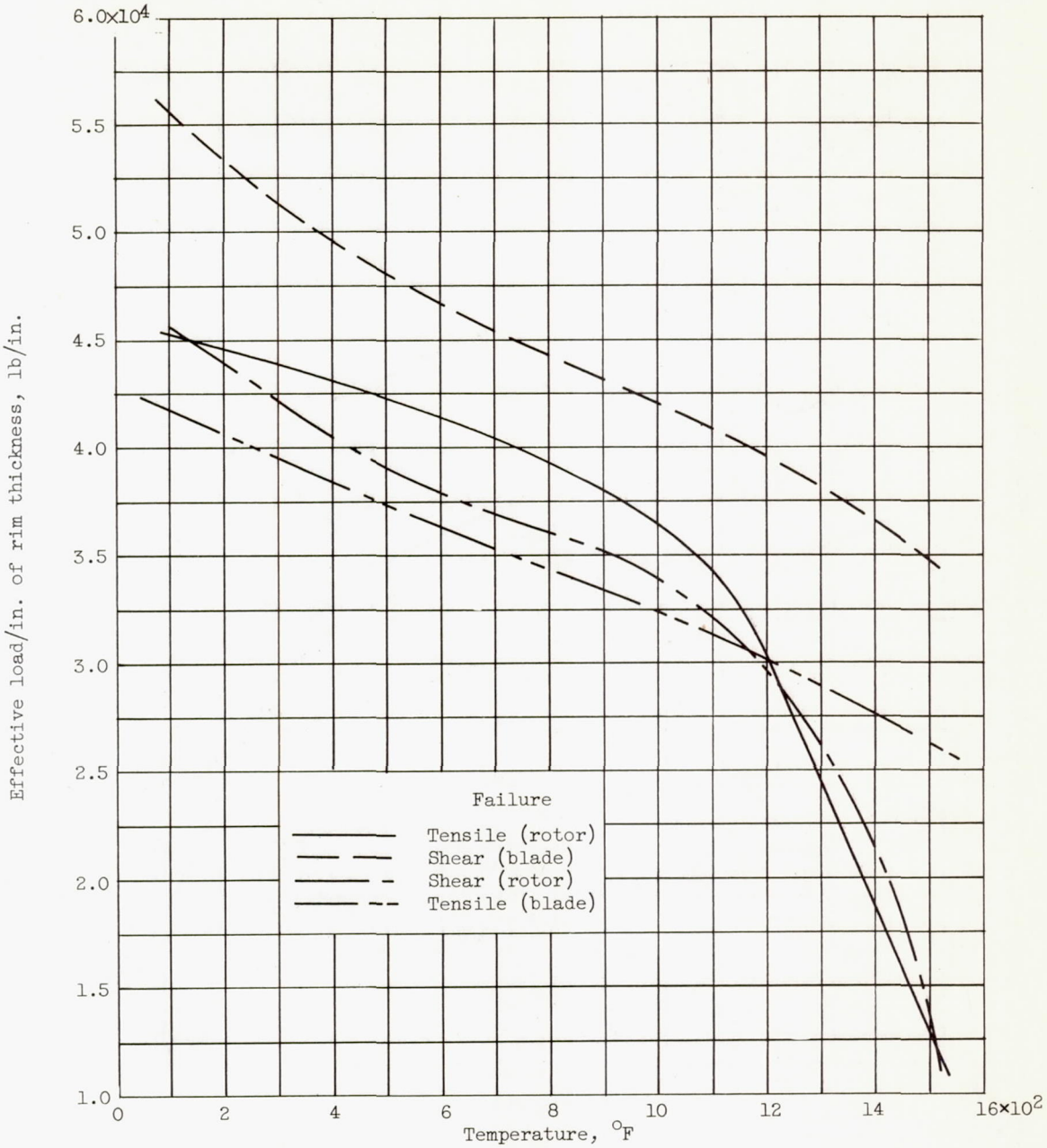

(a) Blade root A.

Figure 13. - Corrected strength data to account for centrifugal field during engine operation.

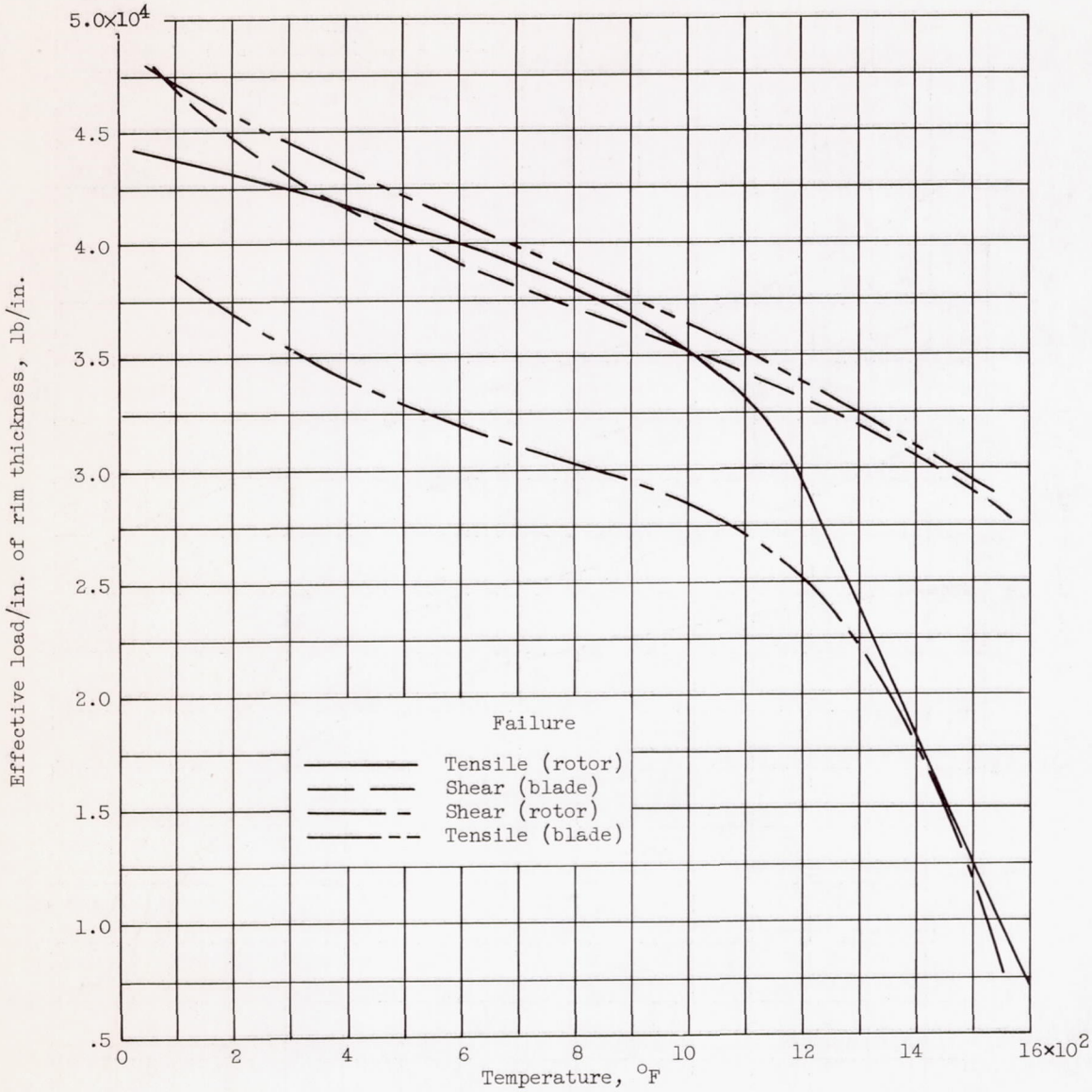

(b) Blade root B.

Figure 13. - Continued. Corrected strength data to account for centrifugal field during engine operation.

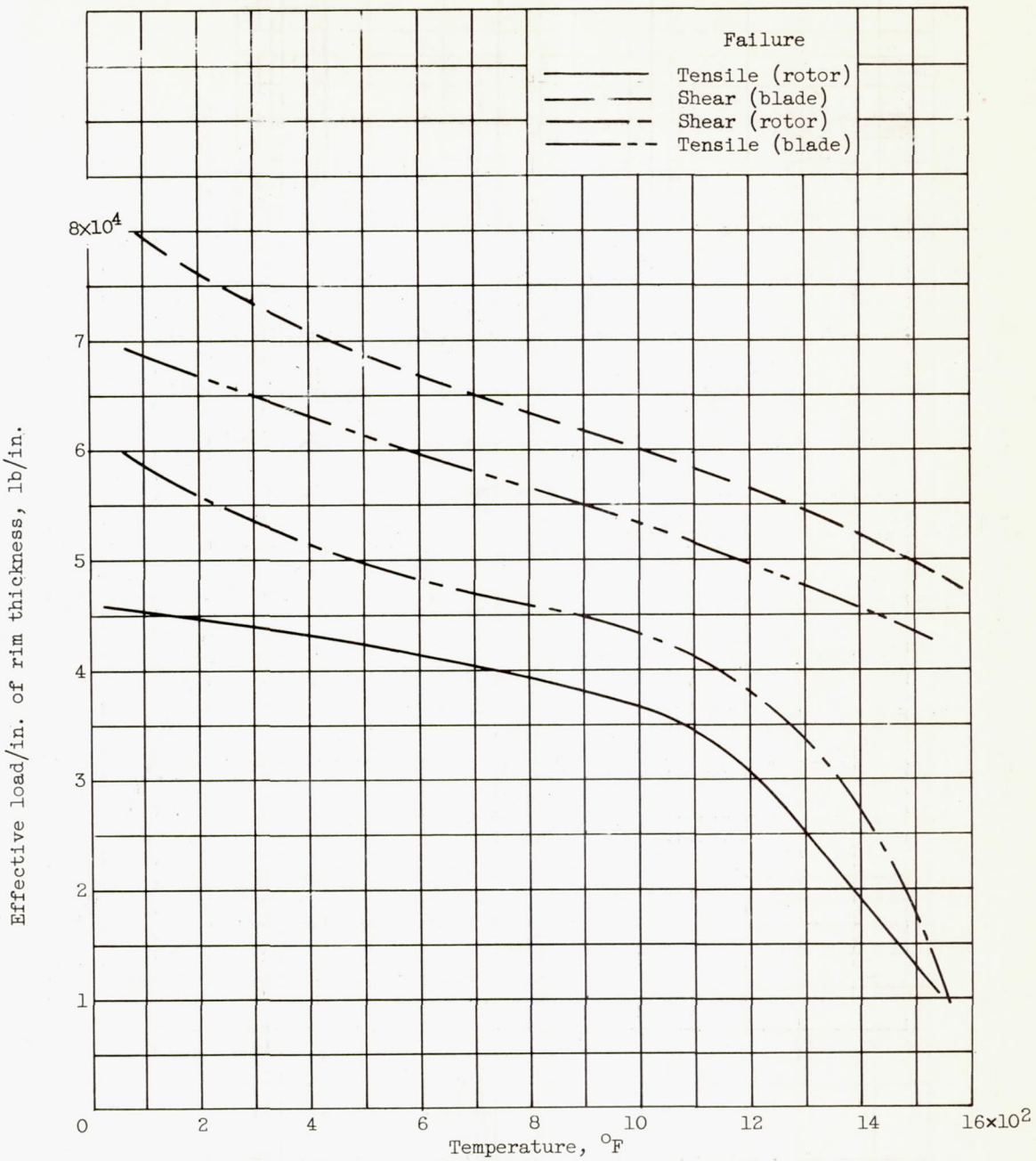

(c) Blade root C.

Figure 13. - Concluded. Corrected strength data to account for centrifugal field during engine operation.

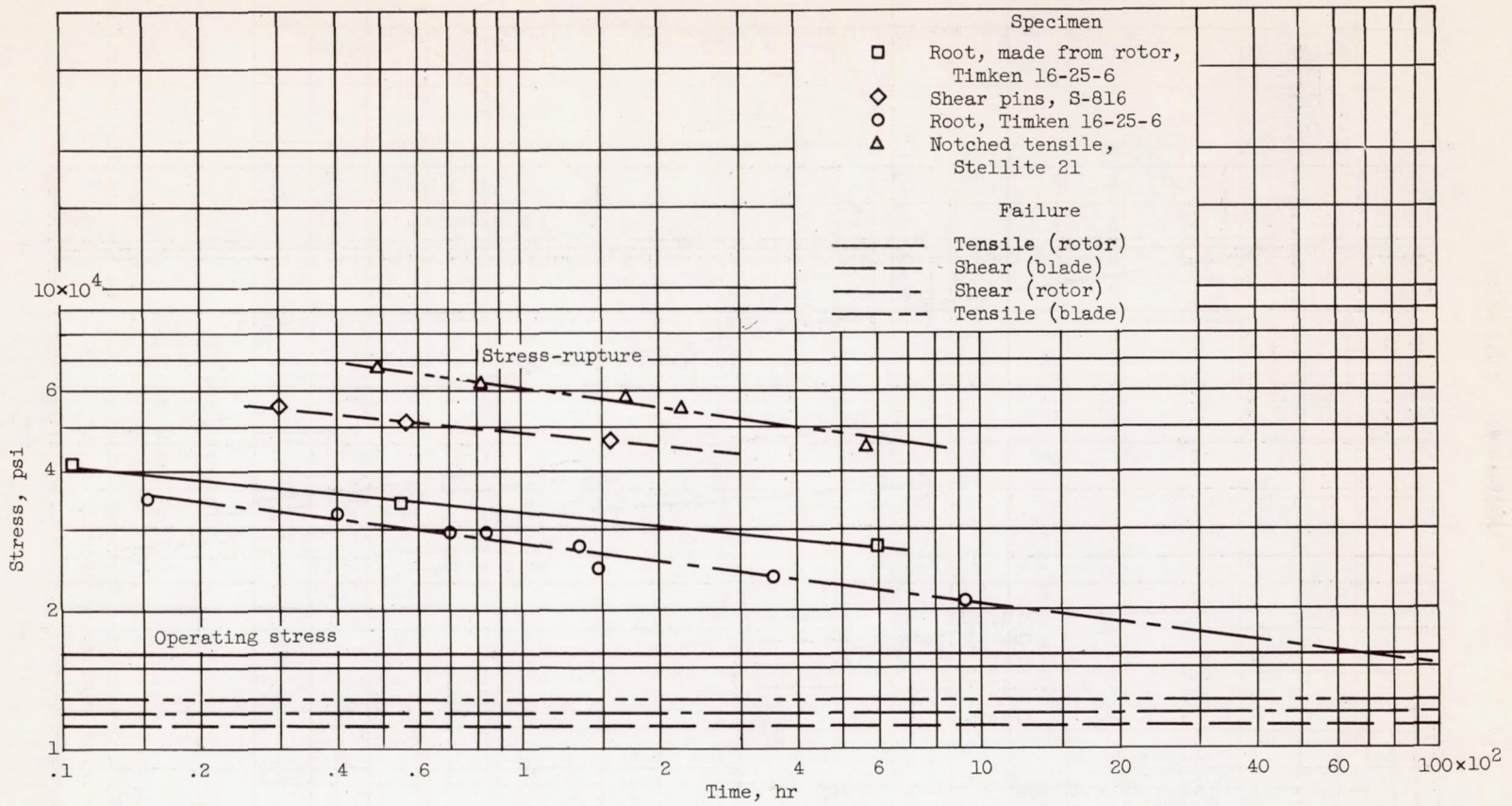

(a) Blade root A.

Figure 14. - Stress-rupture results determined at 1200° F.

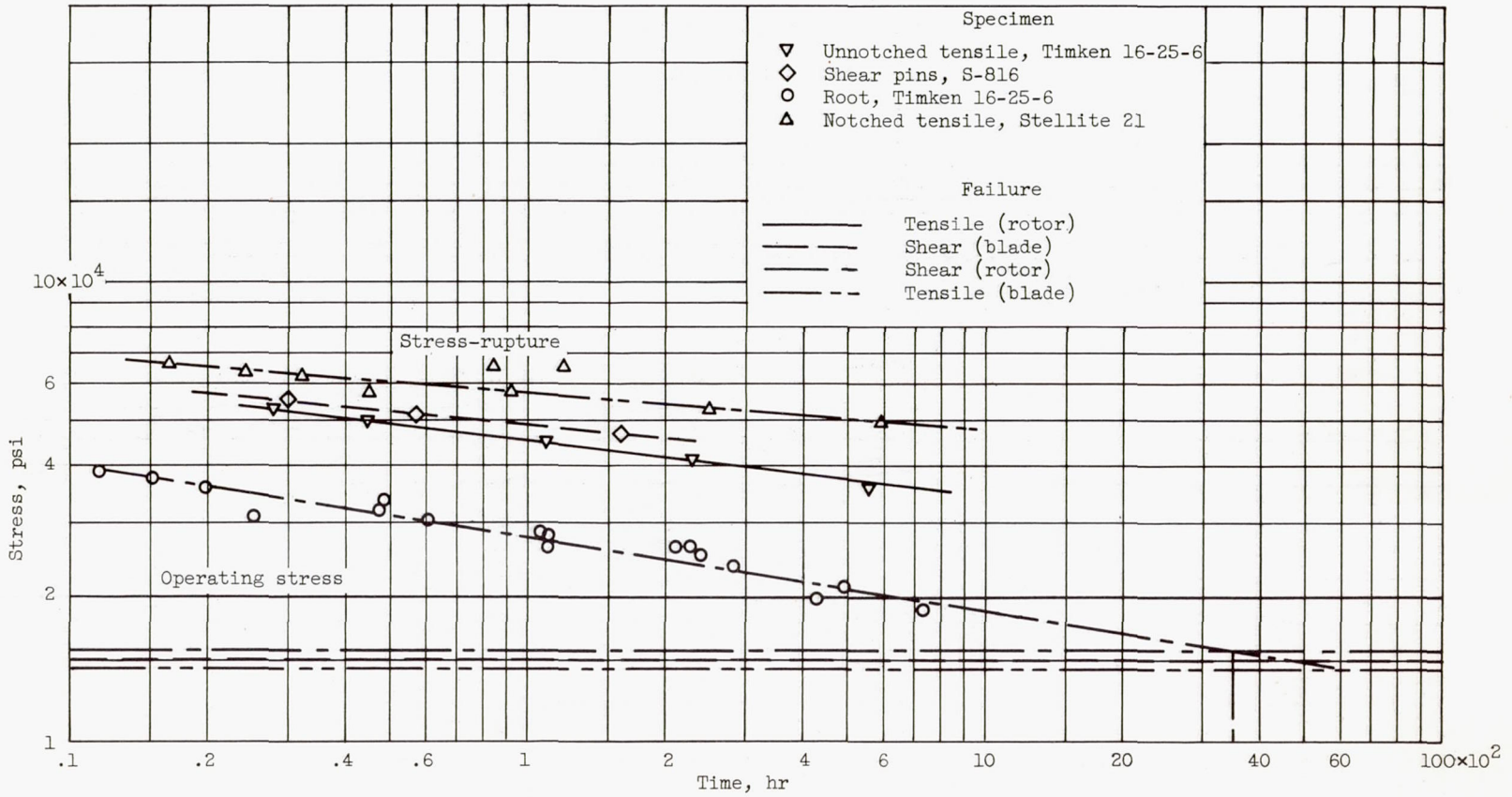

(b) Blade root B.

Figure 14. - Continued. Stress-rupture results determined at 1200° F.

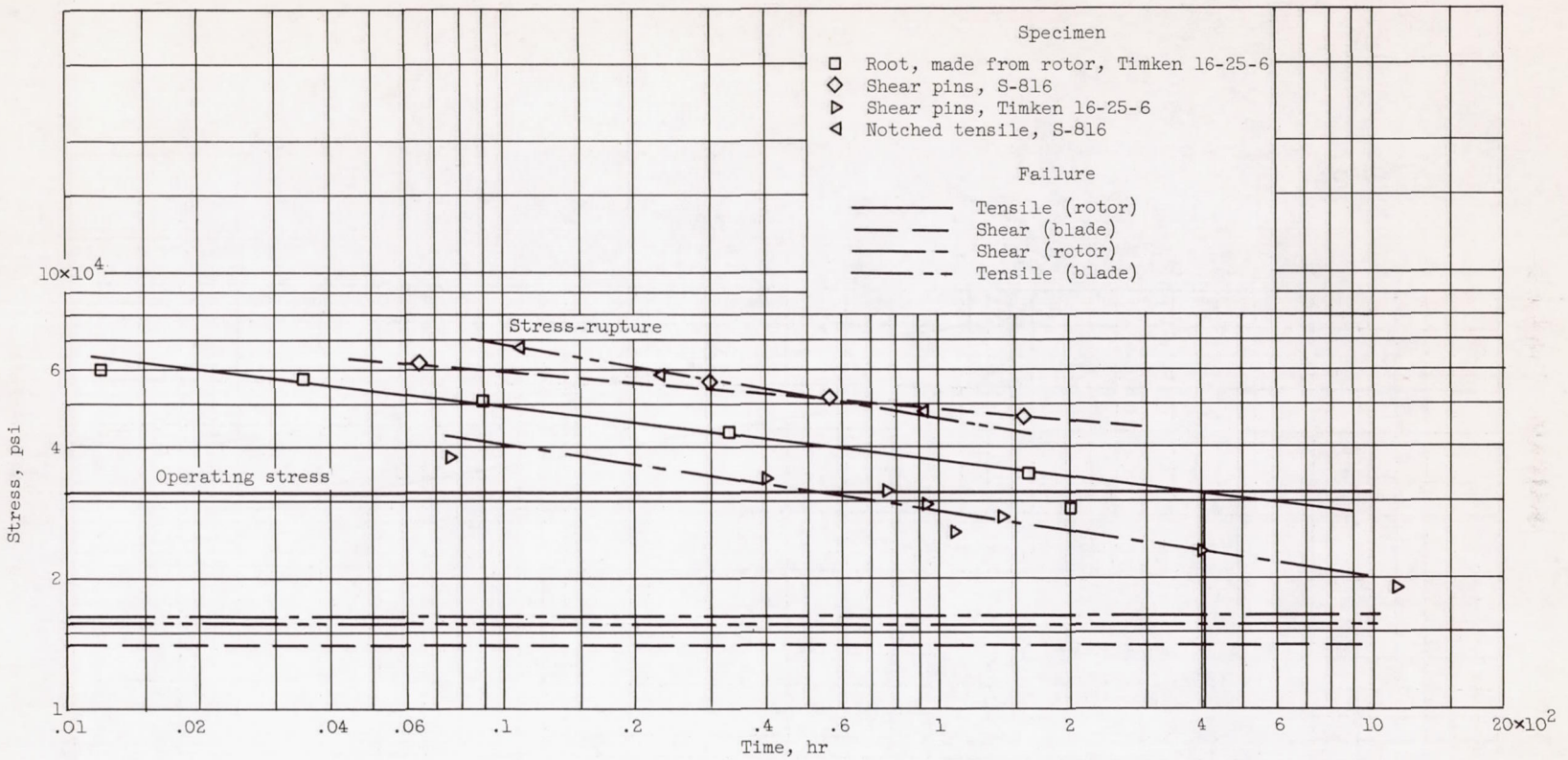

(c) Blade root C.

Figure 14. - Concluded. Stress-rupture results determined at 1200° F.

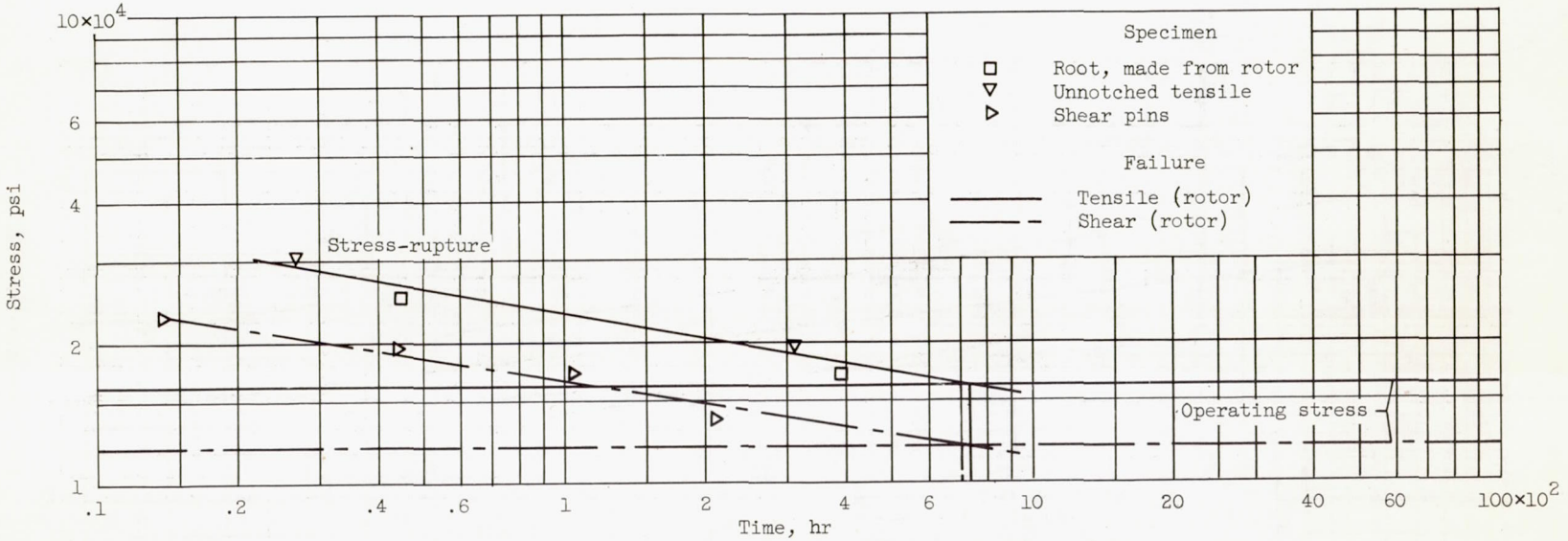

(a) Blade root A.

Figure 15. - Stress-rupture data for turbine rotor at 1350° F. Specimens of Timken 16-25-6.

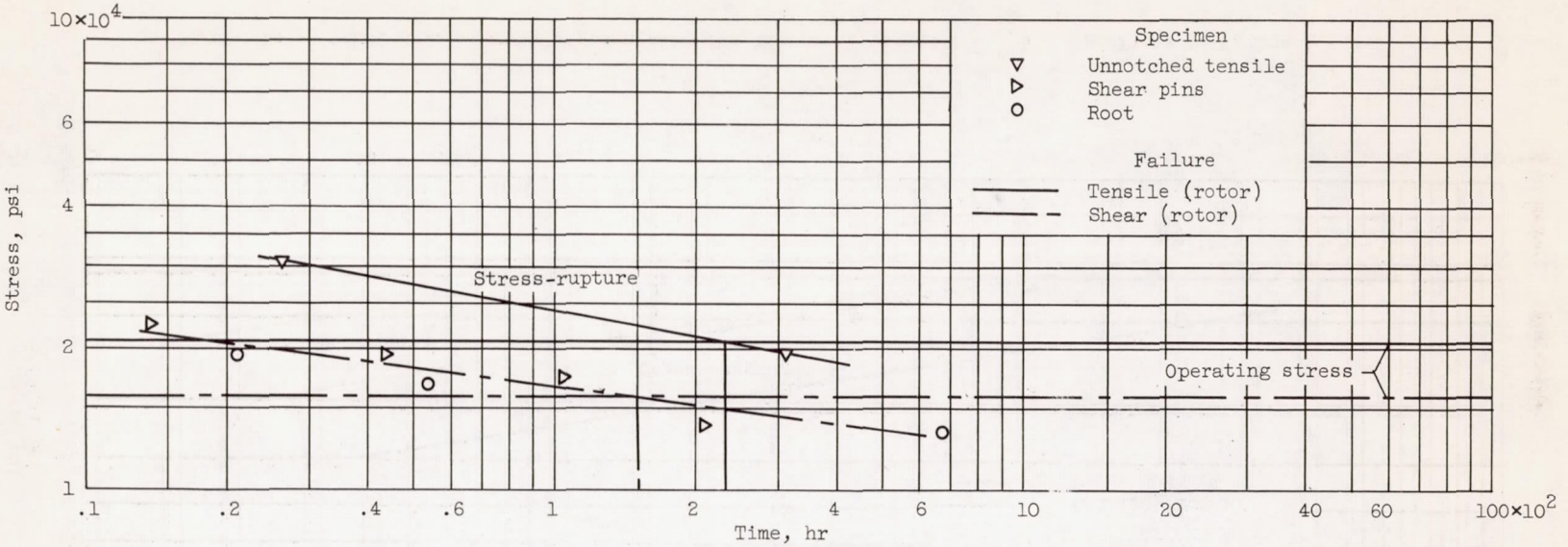

(b) Blade root B.

Figure 15. - Continued. Stress-rupture data for turbine rotor at 1350° F. Specimens of Timken 16-25-6.

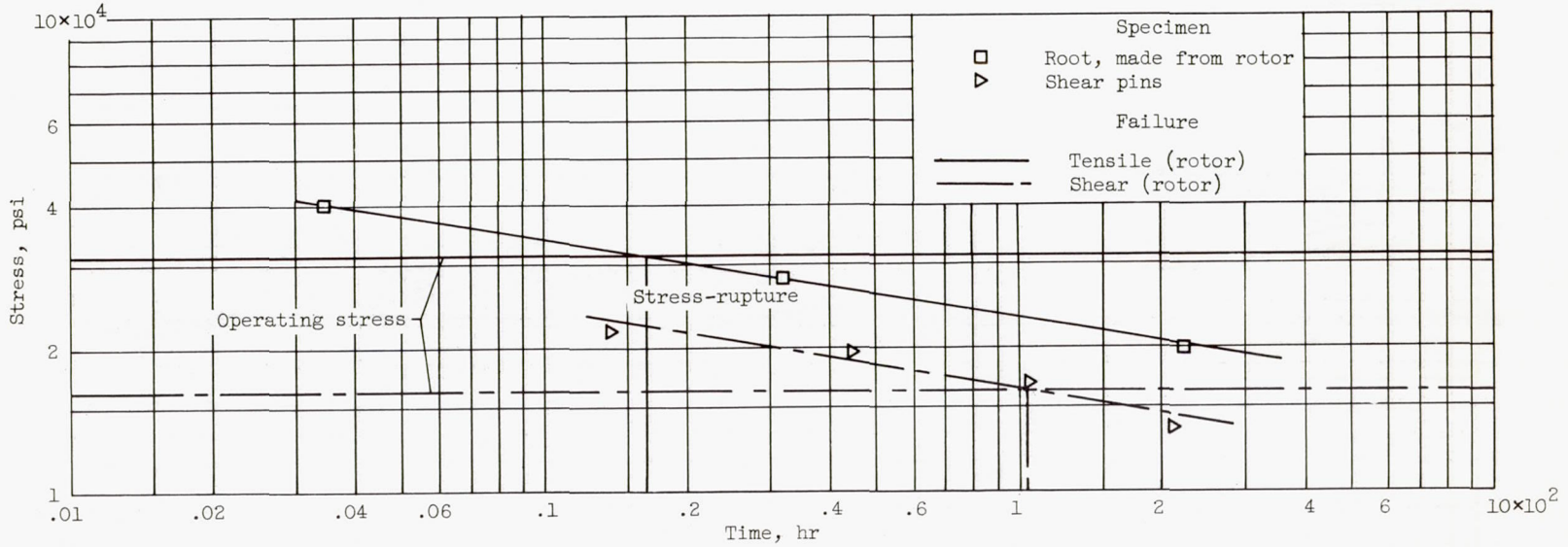

(c) Blade root C.

Figure 15. - Concluded. Stress-rupture data for turbine rotor at 1350° F. Specimens of Timken 16-25-6.

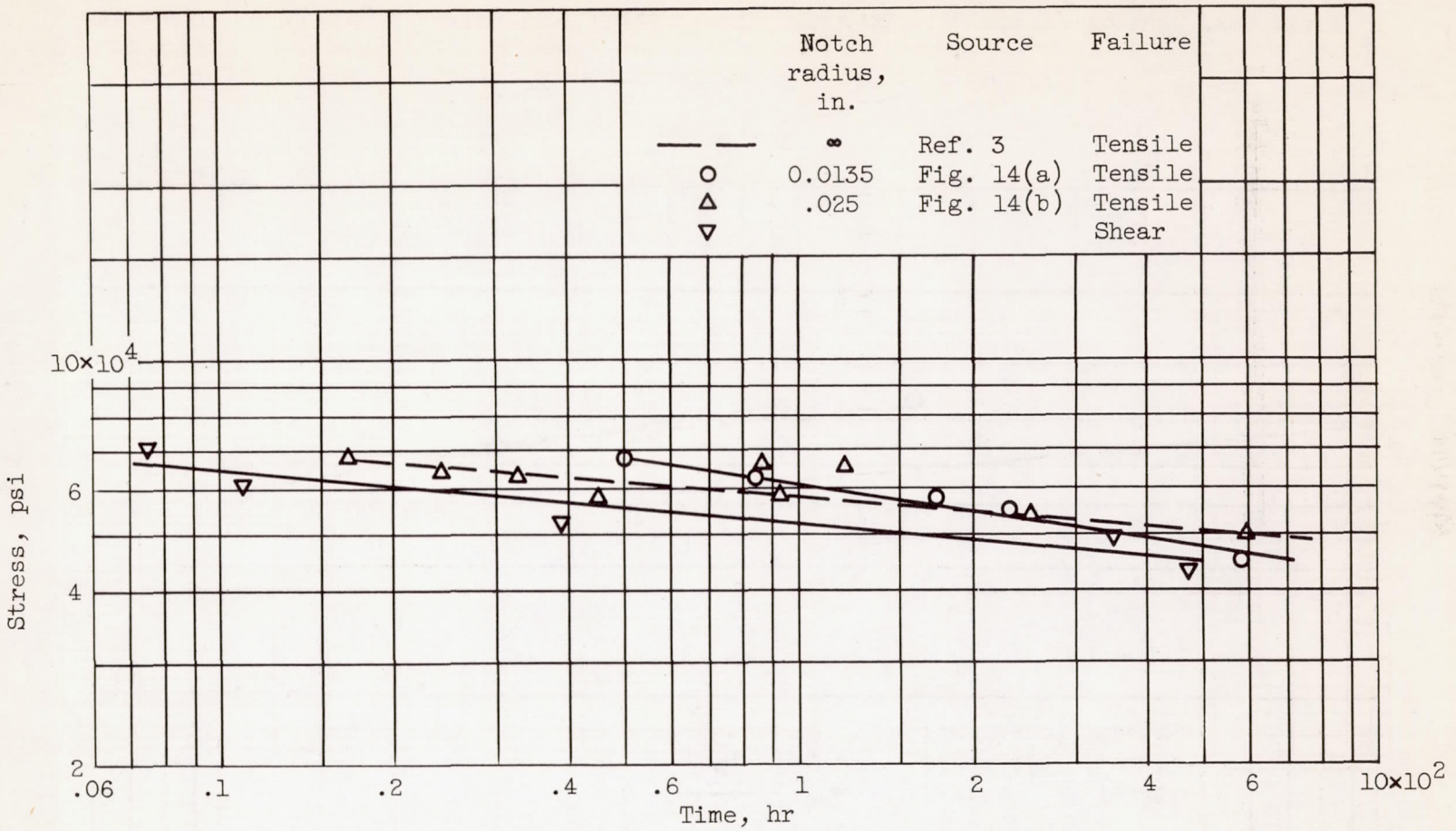

(a) Tensile properties of Stellite 21 at 1200° F.

Figure 16. - Effect of serration fillet radius on stress-rupture properties of turbine blade and rotor materials.

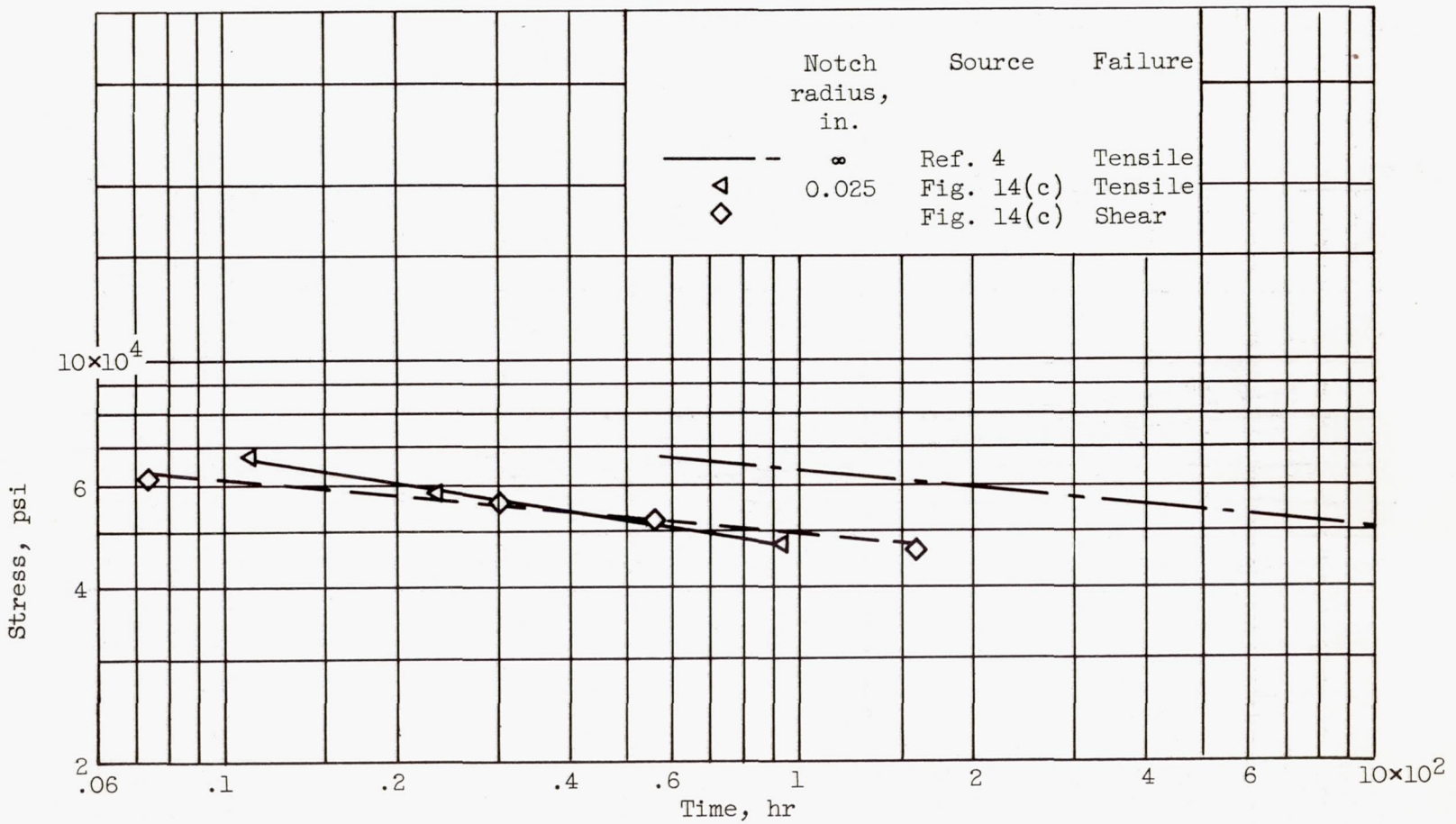

(b) Tensile properties of S-816 at 1200° F.

Figure 16. - Continued. Effect of serration fillet radius on stress-rupture properties of turbine blade and rotor materials.

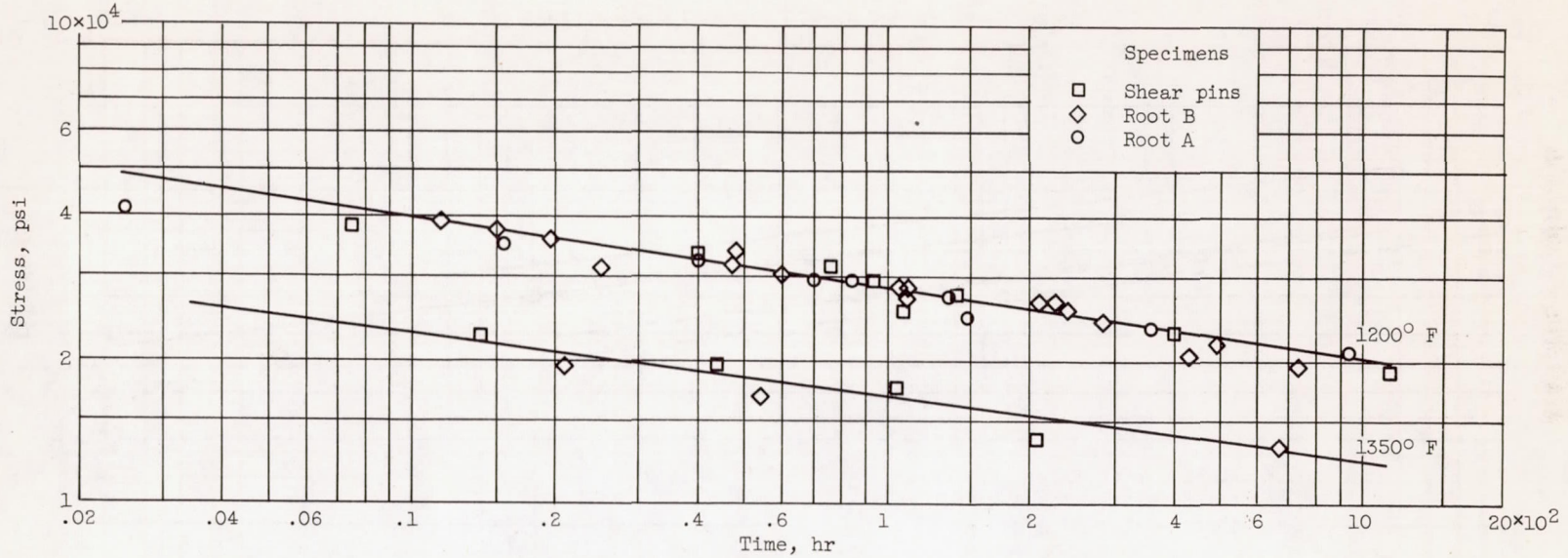

(c) Shear properties of Timken 16-25-6 at 1200° and 1350° F.

Figure 16. - Continued. Effect of serration fillet radius on stress-rupture properties of turbine blade and rotor materials.

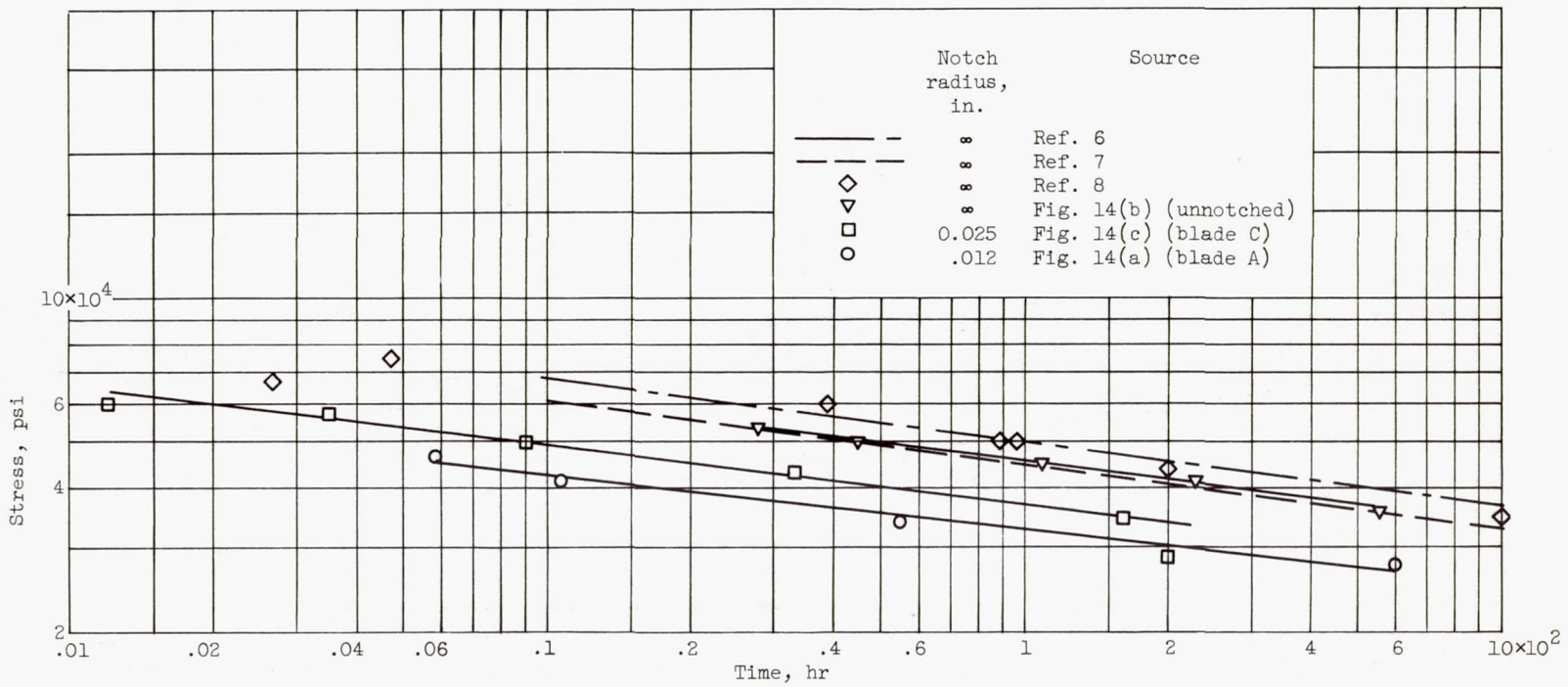

(d) Tensile properties of Timken 16-25-6 at 1200° F.

Figure 16. - Continued. Effect of serration fillet radius on stress-rupture properties of turbine blade and rotor materials.

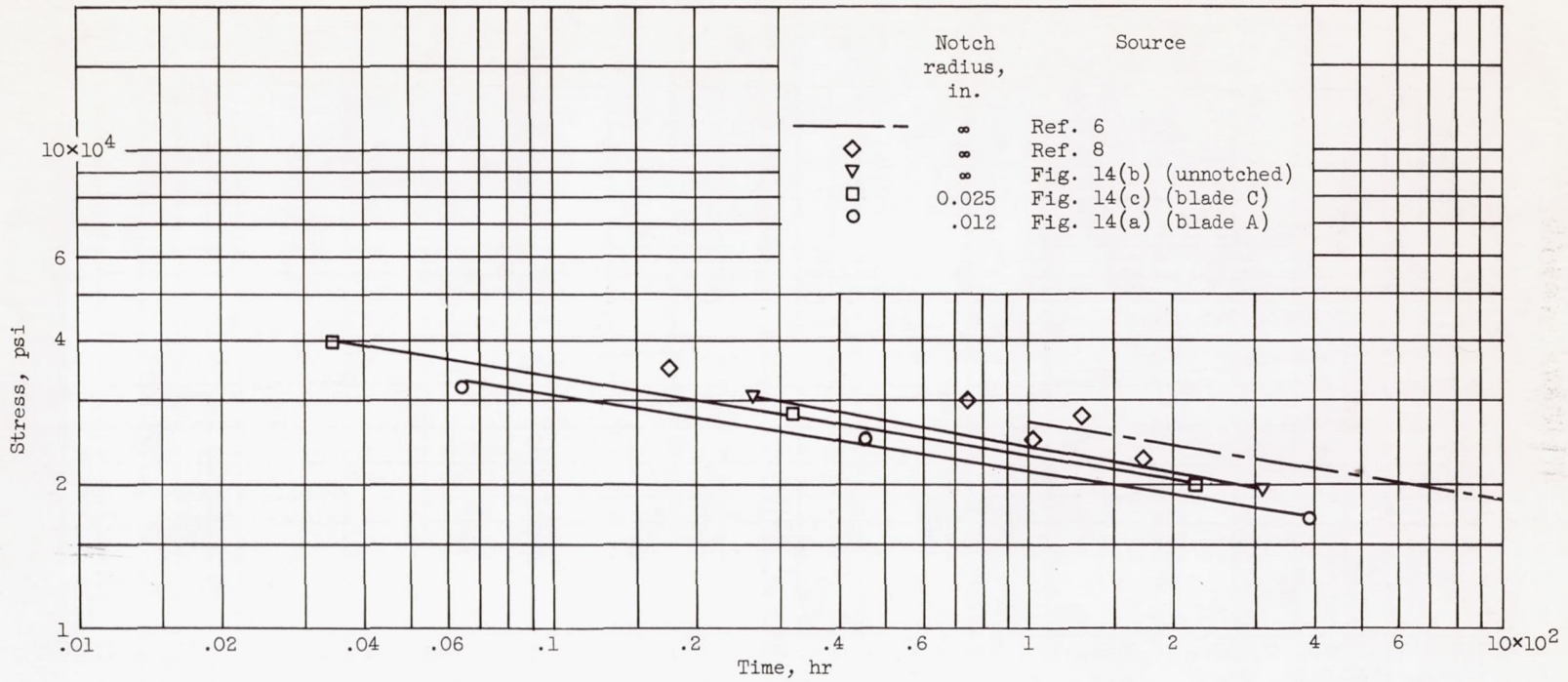

(e) Tensile properties of Timken 16-25-6 at 1350° F.

Figure 16. - Concluded. Effect of serration fillet radius on stress-rupture properties of turbine blade and rotor materials.